Geostationary satellite observations of ozone air quality

Geostationary satellite observations of ozone air quality

A dissertation presented

by

Peter William Zoogman

to

The Department of Earth and Planetary Sciences

in partial fulfillment of the requirements

for the degree of

Doctor of Philosophy

in the subject of

Earth and Planetary Sciences

Harvard University

Cambridge, Massachusetts

August 2013

Dissertation Advisor: Professor Daniel Jacob Peter William Zoogman

Geostationary satellite observations of ozone air quality

Abstract

Ozone in surface air is the primary cause of polluted air in the United States. The current ozone observing network is insufficient either to assess air quality or to fully inform our understanding of the factors controlling tropospheric ozone. This thesis investigates the benefit of an instrument in geostationary orbit for observing near surface ozone using Observing System Simulation Experiments (OSSEs).

An OSSE was performed to define the measurement requirements for geostationary observations of ozone air quality. Hourly observations of ozone from geostationary orbit improve the assimilation considerably relative to daily observation from low earth orbit. There is little propagation of ozone information from the free troposphere to the surface, making instrument sensitivity in the boundary layer is essential. Assimilation of data from a best-case multispectral instrument reduces model error for surface ozone by a factor of two.

A joint assimilation framework was developed to use observations of carbon monoxide as an additional constraint on surface ozone concentrations through exploitation of model error correlations. Ozone-CO error correlations are positive in continental outflow but negative over land on a regional scale. Joint ozone-CO data assimilation provides substantial benefit for informing US ozone air quality if the instrument sensitivity for CO in the boundary layer is greater than that for ozone.

Planned geostationary TEMPO satellite observations of ozone were used in conjunction with complementary surface and low-elevation orbit observations to demonstrate the capability of a future observing system to monitor and attribute air quality exceedances in the

Intermountain West. Assimilation of surface measurements alone does not capture elevated ozone levels. Assimilation of TEMPO geostationary observations greatly improves the assimilated model's ability to reproduce ozone exceedances and attribute them to background influence.

Table of Contents

Chapter 4: Monitoring high-ozone events in the US Intermountain West using TEMPO geostationary satellite observations

List of Figures

Acknowledgements:

I am grateful to my advisor, Daniel Jacob, for his guidance and support through my graduate school journey. It was Daniel who introduced me to the field of atmospheric chemistry and who inspired me to make that field my own. It was a privilege being taught by Daniel; my depth of understanding and inquiry would be less otherwise. Without Daniel I would not be the scientist I am today and this thesis be would be less than it is.

I am indebted to Kelly Chance for his advice and expertise. Most of all, we are all indebted to Kelly for making all our geostationary dreams a reality, and I am excited that he is including me in that reality. Thanks also to Eli Tziperman for being an anchor of my thesis committee and doing it with a smile.

I feel particularly fortunate to have pursued my Ph.D. while a member of the Atmospheric Chemistry Modeling Group at Harvard University. To be part of such a vibrant, intelligent, and collaborative group of scientists has been a tremendous boon. I especially cherish the five years I spent as officemates with Justin Parella for his ideas and his sense of humor. Thanks also go to officemates Moeko Yoshitomi, Patrick Kim, and Shannon Koplitz for their company and support. My appreciation includes many group members past and present, including: Helen Amos, Jenny Fisher, Monika Kopacz, Chris Holmes, Eloise Marias, Chris Miller, Lee Murray, Eric Leibensperger, Philippe Le Sager, Rokjin Park, Bess Sturges-Corbitt, Kevin Wecht, Bob Yantosca, and Lin Zhang. Thank you all (and everyone else) for your assistance, your ideas, and your volleyball.

I have to wholeheartedly thank Chenoweth Moffatt and Sarah Colgan in the EPS department for their time, support, and help in navigating graduate school. They are tremendous assets to the department. Thanks also go to Brenda Mathieu for her time and for keeping our group running.

My work would not have been possible without collaboration with the GEO-CAPE and TEMPO science teams. I gratefully acknowledge the NASA Earth System Science Fellowship for funding my research.

I would like to acknowledge all the support I have been given by my family and friends. Thank you so much to my parents, Carla and Nick, and my sister, Sarah, for your love and for always being there for me. Thank you to my best friends Yves, Shep, Clayton, and Ed for the conversations, meals, and good times that have kept me going. And many thanks to Marianna, for everything.

ὁ δὲ ἀνεξέταστος βίος οὐ βιωτὸς ἀνθρώπῳ

"*The unexamined life is not worth living*"

-Socrates

Chapter 1. Overview

Ozone in the troposphere is of importance as a surface air pollutant, as a greenhouse gas, and as a control of the troposphere's oxidative capacity. It is produced by photochemical oxidation of carbon monoxide (CO) and volatile organic compounds (VOCs) in the presence of nitrogen oxide radicals ($NO_x \equiv NO+NO_2$). These precursors have both natural and anthropogenic sources. Our limited understanding of the factors controlling tropospheric ozone is reflected by the inability of current models to reproduce observed ozone trends over the past century (Mickley et al., 2001; Shindell and Faluvegi, 2002), including the past few decades (Fusco and Logan, 2003).

1.1 Ozone pollution over the United States

Ozone in surface air is harmful to humans and vegetation. Human exposure to ozone causes inflammation in the lower respiratory tract and is associated with increased mortality. 129 million people in the United States breathe hazardous levels of ozone as measured by the National Ambient Air Quality Standard (NAAQS) of 75 ppbv (maximum daily 8-hour average not to be exceeded more than 3 times per year) (EPA, 2012). The US Environmental Protection Agency (EPA) is considering lowering this standard to a value between 60 and 70 ppbv. Although ozone levels are presently decreasing over the eastern US due to emissions controls, ozone has been increasing over the western US. This increase may be attributed to rising background ozone, as evidenced by an increase of free tropospheric ozone over the western US of 0.41 ppbv/year during the past two decades (Cooper et al., 2012).

1.2 Satellite observations of tropospheric composition

Over the past decade, observation of tropospheric ozone and its precursors from space has become an increasingly powerful tool for constraining the ozone budget (Martin et al. 2008). The global continuous observation capability from satellites offers unique insight into the variability of ozone in relation to sources. Current satellite instruments provide reliable measurements of ozone, CO, NO_2, and formaldehyde (Fishman et al. 2008). Assimilation of current satellite ozone measurements has been found to significantly improve modeled ozone concentrations in the free troposphere over North America (Parrington et al. 2008).

All satellite observations of tropospheric ozone and its precursors to date have been from sunsynchronous low-elevation orbit (LEO). These provide a global view, but the return time over a given location is too long to track the low-altitude (boundary layer) variability relevant to ozone air quality (Fishman et al. 2008). Furthermore, current satellite observations have poor sensitivity in the boundary layer, in the UV because of molecular scattering and in the TIR because of lack of thermal contrast.

An instrument in geostationary orbit could provide hourly data covering a continental scale (Fishman et al., 2012), representing a transformative development for observing air quality from space. The GEO-CAPE (Geostationary Coastal And Pollution Events) mission was recommended to NASA in the Decadal Survey (National Research Council, 2007). This thesis evolved from the need to demonstrate the benefit of geostationary observations and determine measurement requirements and observation strategies for GEO-CAPE and other future geostationary missions. Informed by this thesis, a global constellation of geostationary satellite missions targeted at air quality is planned to launch in 2018-2019 including TEMPO (Tropospheric Emissions: Monitoring of Pollution) over North America

(Chance et al., 2012), SENTINEL-4 over Europe (Ingmann et al., 2012), and GEMS over East Asia (Bak et al., 2013).

1.3 Research objectives and approach

This thesis aims to determine the potential of geostationary satellite instruments to observe and constrain ozone air quality through data assimilation, and in this manner to contribute to the design of future geostationary missions and enable exploitation of their data. I address the following specific questions:

- What measurement requirements must be met for geostationary observations to accurately constrain ozone in the boundary layer?
- Can concurrent geostationary measurements of CO improve monitoring of surface ozone air quality through a joint assimilation?
- What will be the ability of geostationary observations to monitor and attribute air quality exceedances in the Intermountain West and thus guide future air quality policy?
- What is the additional benefit of these observations in the context of the existing ozone monitoring network of surface sites?

To address these questions I conduct Observing System Simulation Experiments (OSSEs). In the OSSE framework, I generate synthetic ozone data from a chemical transport model (CTM) to represent the "true" atmosphere. I then examine the capability of proposed instruments and observing strategies to deliver on scientific objectives through formal data assimilation into an independent CTM taken as forward model. OSSEs are the standard approach to quantify the potential benefit of a proposed observation platform toward a scientific goal (Lord et al. 1997). I use the GEOS-

Chem CTM (Bey et al., 2001) as the forward model. CTMs used to provide the "true" atmosphere include MOZART (Fiore et al., 2011), AM3-Chem (Lin et al., 2012), and a version of GEOS-Chem with independent meteorological data.

To perform the data assimilation, I implement a Kalman filter in the GEOS-Chem CTM. A Kalman filter provides the best estimate of the state at a given time step using measurements at that time step and information from previous time steps (Rodgers 2000). The optimization depends on the error covariance matrices in the observations and the model as well as the averaging kernel matrix of the observations. The inclusion of spatial and cross-species model error correlations is a critical advancement of my data assimilation system. Model errors are quantified by comparison to *in situ* measurements from the Clean Air Status and Trends Network (CASTNet; www.epa.gov/castnet) ground stations, the ICARTT (Singh et al., 2006; Fehsenfeld et al., 2006) aircraft campaign, and the IONS (Cooper et al. 2011) ozonesonde network.

1.4 Summary of results

Chapter 2 describes an Observing System Simulation Experiment (OSSE) to test the ability of geostationary satellite measurements of ozone in different spectral regions to constrain surface ozone concentrations through data assimilation. This was done to define the measurement requirements for geostationary observations of ozone air quality. Instruments using different spectral combinations of UV (290-340 nm), Vis (560-620 nm), and thermal IR (TIR, 9.6 μm) are analyzed. Hourly observations of ozone from geostationary orbit improve the assimilation considerably relative to daily observation from low earth orbit. UV+Vis and UV+TIR spectral combinations improve greatly the information on surface ozone relative to UV

alone. Assimilation of data from a UV+Vis+TIR instrument reduces the GEOS-Chem error for surface ozone by a factor of two.

Chapter 3 presents an innovative approach to assimilating ozone air quality from space using observations of carbon monoxide as an additional error correlation constraint in a joint ozone-CO assimilation. Boundary layer sensitivity is easier to achieve for satellite observations of CO than for satellite observations of ozone. A paired-model analysis of ozone-CO error correlations in the boundary layer over North America in summer indicates positive error correlations in continental outflow but negative regional-scale error correlations over land, the latter reflecting opposite sensitivities of ozone and CO to boundary layer depth. There is substantial benefit from joint ozone-CO data assimilation in informing US ozone air quality if the instrument sensitivity for CO in the boundary layer is greater than that for ozone. A high-quality geostationary measurement of CO could potentially relax the requirements for boundary layer sensitivity of the ozone measurement. Successful implementation of a joint assimilation depends on accurate characterization of ozone-CO error correlations.

Chapter 4 examines the ability of the future geostationary satellite TEMPO (Tropospheric Emissions: Monitoring of Pollution) to monitor and attribute air quality exceedances in the Intermountain West. TEMPO observations were considered in the context of complementary ozone measurements provided by surface stations and currently planned low-elevation (LEO) orbit instruments. We show that assimilation of surface measurements improves modeled surface ozone in the Intermountain West but does not capture elevated levels due to lack of information in the free troposphere and sparse spatial coverage. Assimilation of TEMPO geostationary observations greatly improves the assimilated model's ability to reproduce ozone exceedances and attribute them to background influence.

References:

Bak, J., Kim, J.H., Liu, X., Chance, K., Kim, J., 2013. Evaluation of ozone profile and tropospheric ozone retrievals from GEMS and OMI spectra. Atmospheric Measurement Techniques 6, 239-249.

Bey, I., Jacob, D., Yantosca, R., Logan, J., Field, B., Fiore, A., Li, Q., Liu, H., Mickley, L., Schultz, M., 2001. Global modeling of tropospheric chemistry with assimilated meteorology: Model description and evaluation. Journal of Geophysical Research-Atmospheres 106, 23073-23095.

Chance, K., Lui, X., Suleiman, R.M., Flittner, D.E., Janz, S.J., 2012. Tropspheric Emissions: Monitoring of Pollution (TEMPO). Abstract A31B-0020 presented at the 2012 AGU Fall Meeting

Cooper, O.R., Oltmans, S.J., Johnson, B.J., Brioude, J., Angevine, W., Trainer, M., Parrish, D.D., Ryerson, T.R., Pollack, I., Cullis, P.D., Ives, M.A., Tarasick, D.W., Al-Saadi, J., Stajner, I., 2011. Measurement of western US baseline ozone from the surface to the tropopause and assessment of downwind impact regions. Journal of Geophysical Research-Atmospheres 116, D00V03.

Cooper, O.R., Gao, R., Tarasick, D., Leblanc, T., Sweeney, C., 2012. Long-term ozone trends at rural ozone monitoring sites across the United States, 1990-2010. Journal of Geophysical Research-Atmospheres 117, D22307.

Fehsenfeld, F.C., Ancellet, G., Bates, T.S., Goldstein, A.H., Hardesty, R.M., Honrath, R., Law, K.S., Lewis, A.C., Leaitch, R., McKeen, S., Meagher, J., Parrish, D.D., Pszenny, A.A.P., Russell, P.B., Schlager, H., Seinfeld, J., Talbot, R., Zbinden, R., 2006. International consortium for atmospheric research on transport and transformation (ICARTT): North america to europe - overview of the 2004 summer field study. Journal of Geophysical Research-Atmospheres 111, D23S01.

Fiore, A.M., Levy, H., Jaffe, D.A., 2011. North American isoprene influence on intercontinental ozone pollution. Atmospheric Chemistry and Physics 11, 1697-1710.

Fishman, J., Bowman, K.W., Burrows, J.P., Richter, A., Chance, K.V., Edwards, D.P., Martin, R.V., Morris, G.A., Pierce, R.B., Ziemke, J.R., Al-Saadi, J.A., Creilson, J.K., Schaack, T.K., Thompson, A.M., 2008. Remote sensing of tropospheric pollution from space. Bulletin of the American Meteorological Society 89, 805-821.

Fishman, J., Iraci, L.T., Al-Saadi, J., Chance, K., Chavez, F., Chin, M., Coble, P., Davis, C., DiGiacomo, P.M., Edwards, D., Eldering, A., Goes, J., Herman, J., Hu, C., Jacob, D.J., Jordan, C., Kawa, S.R., Key, R., Liu, X., Lohrenz, S., Mannino, A., Natraj, V., Neil, D., Neu, J., Newchurch, M., Pickering, K., Salisbury, J., Sosik, H., Subramaniam, A., Tzortziou, M., Wang, J., Wang, M., 2012. The United States' next generation of

atmospheric composition and coastal ecosystem measurements NASA's geostationary coastal and air pollution events (GEO-CAPE) mission. Bulletin of the American Meteorological Society 93, 1547-+.

Fusco, A.C., Logan, J.A., 2003. Analysis of 1970-1995 trends in tropospheric ozone at Northern Hemisphere midlatitudes with the GEOS-CHEM model. Journal of Geophysical Research-Atmospheres 108.

Ingmann, P., Veihelmann, B., Langen, J., Lamarre, D., Stark, H., Courreges-Lacoste, G.B., 2012. Requirements for the GMES atmosphere service and ESA's implementation concept: Sentinels-4/-5 and-5p. Remote Sensing of Environment 120, 58-69.

Lin, M., Fiore, A.M., Cooper, O.R., Horowitz, L.W., Langford, A.O., Levy,Hiram,,II, Johnson, B.J., Naik, V., Oltmans, S.J., Senff, C.J., 2012. Springtime high surface ozone events over the western United States: Quantifying the role of stratospheric intrusions. Journal of Geophysical Research-Atmospheres 117, D00V22.

Lord, S.J., Kalnay E., Daley R., Emmitt G.D., Atlas R., 1997. Using OSSEs in the design of future generation integrated observing systems. Preprints, 1st Symposium on Integrated Observing Systems, Long Beach, CA, AMS, 45-47.

Martin, R.V., 2008. Satellite remote sensing of surface air quality. Atmospheric Environment 42, 7823-7843.

Mickley, L.J., Jacob, D.J., Rind, D., 2001. Uncertainty in preindustrial abundance of tropospheric ozone: Implications for radiative forcing calculations. Journal of Geophysical Research-Atmospheres 106, 3389-3399.

National Research Council, 2007. Earth Science and Applications from Space: National Imperatives for the Next Decade and Beyond. Washington, D.C.: National Academy Press.

Parrington, M., Jones, D.B.A., Bowman, K.W., Horowitz, L.W., Thompson, A.M., Tarasick, D.W., Witte, J.C., 2008. Estimating the summertime tropospheric ozone distribution over North America through assimilation of observations from the Tropospheric Emission Spectrometer. Journal of Geophysical Research-Atmospheres 113.

Rodgers, C.D., 2000. Inverse methods for atmospheric sounding. River Edge, New Jersey: World Scientific.

Shindell, D.T., Faluvegi, G., 2002. An exploration of ozone changes and their radiative forcing prior to the chlorofluorocarbon era. Atmospheric Chemistry and Physics 2, 363-374.

Singh, H.B., Brune, W.H., Crawford, J.H., Jacob, D.J., Russell, P.B., 2006. Overview of the summer 2004 intercontinental chemical transport experiment - North America (INTEX-A). Journal of Geophysical Research-Atmospheres 111, D24S01.

United States Environmental Protection Agency, 2012. Welfare Risk and Exposure Assessment for Ozone.

Chapter 2. Ozone air quality measurement requirements for a geostationary satellite mission

[Zoogman, P., Jacob, D.J., Chance, K., Zhang, L., Le Sager, P., Fiore, A.M., Eldering, A., Liu, X., Natraj, V., Kulawik, S.S., 2011. Ozone air quality measurement requirements for a geostationary satellite mission. Atmospheric Environment 45, 7143-7150. Copyright 2011 Atmospheric Environment]

Abstract

We conduct an Observing System Simulation Experiment (OSSE) to test the ability of geostationary satellite measurements of ozone in different spectral regions to constrain surface ozone concentrations through data assimilation. Our purpose is to define instrument requirements for the NASA GEO-CAPE geostationary air quality mission over North America. We consider instruments using different spectral combinations of UV (290-340 nm), Vis (560-620 nm), and thermal IR (TIR, 9.6 μm). Hourly ozone data from the MOZART global 3-D chemical transport model (CTM) are taken as the "true" atmosphere to be sampled by the instruments for July 2001. The resulting synthetic data are assimilated in the GEOS-Chem CTM using a Kalman filter. The MOZART and GEOS-Chem CTMs have independent heritages and use different assimilated meteorological data sets for the same period, making for an objective OSSE. We show that hourly observations of ozone from geostationary orbit improve the assimilation considerably relative to daily observation from low earth orbit, and that

broad observation over the ocean is unnecessary if the objective is to constrain surface ozone distribution over land. We also show that there is little propagation of ozone information from the free troposphere to the surface, so that instrument sensitivity in the boundary layer is essential. UV+Vis and UV+TIR spectral combinations improve greatly the information on surface ozone relative to UV alone. UV+TIR is preferable under high-sensitivity conditions with strong thermal contrast at the surface, but UV+Vis is preferable under low-sensitivity conditions. Assimilation of data from a UV+Vis+TIR instrument reduces the GEOS-Chem error for surface ozone by a factor of two. Observation in the TIR is critical to obtain ozone information in the upper troposphere relevant to climate forcing.

2.1 Introduction

Ozone in the troposphere is of importance as a surface air pollutant, as a greenhouse gas, and as the precursor of OH, the main atmospheric oxidant. It is produced by photochemical oxidation of carbon monoxide (CO) and volatile organic compounds (VOCs) in the presence of nitrogen oxide radicals ($NO_x \equiv NO+NO_2$). These precursors have both natural and anthropogenic sources. The dependence of ozone production on its precursors is complex and highly non-linear, and involves a continuum of time scales ranging from milliseconds to years. Our limited understanding of the factors controlling tropospheric ozone is reflected by the inability of current models to reproduce observed ozone trends over the past century (Mickley et al., 2001; Shindell and Faluvegi, 2002), including the past few decades (Fusco and Logan, 2003).

Over the past decade, observation of tropospheric ozone and its precursors from space

has become an increasingly powerful tool for understanding the ozone budget (Martin 2008). Current satellite instruments provide reliable measurements of ozone, CO, NO_2, and formaldehyde (HCHO) (Fishman et al. 2008). The Aura satellite includes direct measurements of tropospheric ozone by two instruments measuring in different spectral regions: the Tropospheric Emission Spectrometer (TES) in the thermal infrared (TIR) (Beer 2006) and the Ozone Monitoring Instrument (OMI) in the UV (Levelt et al. 2006, Liu et al., 2009). Consistency between TES and OMI measurements has been demonstrated (Zhang et al. 2010). These data have been used to constrain models of tropospheric ozone, including the source from biomass burning (Jones et al. 2006), intercontinental transport (Zhang et al. 2006), and greenhouse radiative forcing (H. Worden et al. 2008). Assimilation of TES ozone has been found to significantly improve modeled ozone concentrations in the free troposphere over North America (Parrington et al. 2008).

All satellite observations of tropospheric ozone and its precursors so far have been from sunsynchronous low earth orbit (LEO). They provide a global view but the return time over a given location is too long to track the low-altitude (boundary layer) variability relevant to ozone air quality (Fishman et al. 2008). An instrument in geostationary orbit could provide hourly data covering a continental scale (Campbell and Fishman 2008), allowing monitoring of the progression of pollution events and the diurnal evolution of sources and chemistry. This would represent a transformative development for observing air quality from space. GEO-CAPE (Geostationary Coastal And Pollution Events), a NASA satellite mission planned for launch in the next decade, holds much promise in this regard (National Research Council (NRC), 2007). Parallel plans for geostationary missions directed at air quality are presently underway in Europe (Committee on Earth Observation Satellites, 2009) and in Korea (Lee et al. 2010).

Design of GEO-CAPE is at an early stage. The specific measurement requirements and observation strategy have not yet been determined. An Observing System Simulation Experiment (OSSE) framework is useful for this purpose. GEO-CAPE observations are intended to be assimilated into models to improve understanding of air quality and aid in its forecasting; an OSSE can address the question of how much information these observations will actually provide. In the OSSE framework, we generate synthetic ozone data from a chemical transport model (CTM) to represent the "true" atmosphere. We then examine the capability of different possible instrument configurations and observing strategies to deliver on the proposed scientific objectives through formal data assimilation into an independent CTM taken as forward model. OSSEs are the standard approach to quantify the potential benefit of a proposed observation platform toward a scientific goal (Lord et al. 1996). An OSSE study by Edwards et al. (2009) previously showed that geostationary CO observations would be significantly more effective than LEO observations in improving the ability of models to describe pollution events on a synoptic scale.

Here we present an OSSE for ozone air quality observations from geostationary orbit over North America, focusing on the potential capability of instruments measuring in different combinations of spectral ranges: UV+Visible (Vis), UV+TIR, and UV+Vis+TIR. We generate synthetic observations for July 2001 by having these different instruments "observe" 3-D ozone fields from the MOZART CTM (Fiore et al. 2011). These synthetic observations are then assimilated into the GEOS-Chem CTM (Park et al. 2006, Wang et al. 2009) and we quantify how much information each instrument configuration provides to reduce the difference between GEOS-Chem and the "true" MOZART atmosphere. The MOZART and GEOS-Chem CTMs have different heritages and use different assimilated

meteorological fields for the same period, thus providing an OSSE with realistic error. Both are global CTMs, which is necessary because smoothing errors from satellite observations result in upper tropospheric information (transported on a global scale) influencing the lower tropospheric retrievals. They still have sufficient horizontal resolution to describe transport on synoptic scales, and sufficient vertical resolution to describe mass exchange between the free troposphere and the surface.

2.2 Ozone air quality measurements from GEO-CAPE

The NASA GEO-CAPE geostationary mission over North America was recommended by the 2007 NRC *Earth Science Decadal Survey* (NRC 2007) as one of 14 top-priority satellite missions for NASA in the coming decade. GEO-CAPE has both an air quality and a coastal ecosystems component. Primary objectives of the air quality component include the mapping of emissions for ozone and aerosol precursors, the observation of ozone and aerosols with sensitivity near the surface, and the quantification of ozone and aerosol radiative forcing.

A major challenge for GEO-CAPE is the measurement of ozone with sensitivity near the surface. Direct satellite retrievals of tropospheric ozone have been made from solar backscattered UV spectra in the Hartley-Huggins bands (290-340 nm) (Liu et al. 2005, 2010) and from TIR emission in the 9.6 μm ν_3 band (Beer et al. 2006). These have poor sensitivity in the boundary layer, in the UV because of molecular scattering and in the TIR because of lack of thermal contrast. UV and TIR instruments have similar vertical sensitivities for tropospheric ozone as indicated by their averaging kernel matrices (Zhang et al. 2010). Theoretical studies have suggested that boundary layer sensitivity to ozone could be improved by using multi-spectral approaches involving UV+TIR (J. Worden et al. 2007, Landgraf and Hasekamp 2007)

or UV plus the weak Vis Chappuis band (560-620 nm) (Chance et al., 1997; Liu et al. 2005).

The retrieval sensitivity of vertical concentration profiles retrieved from satellite spectra can be expressed as an averaging kernel matrix **A** relating the retrieved profile $\mathbf{x}'$ to the true profile **x** and an *a priori* profile $\mathbf{x_a}$:

$$\mathbf{x}' = \mathbf{x_a} + \mathbf{A}(\mathbf{x} - \mathbf{x_a}) + \varepsilon \quad (2.1)$$

where ε is the random spectral measurement error (Rodgers, 2000). Averaging kernel matrices for tropospheric ozone profile retrievals in the different spectral combinations described above have been produced by the GEO-CAPE Simulation Team (Natraj et al. 2011). We consider here clear-sky averaging kernel matrices from four spectral combinations: UV, UV+Vis, UV+TIR, and UV+Vis+TIR. The UV (290-340 nm) and Vis (560-620 nm) candidate sensors each have a spectral resolution of 0.4 nm and a signal to noise ratio three times that of OMI. The TIR (980-1070 cm^{-1}) sensor has a spectral resolution of 0.1 cm^{-1} and a signal to noise ratio three times that of TES. The averaging kernel matrices used in this analysis do not include the impacts of clouds and aerosols. Clouds and aerosols are expected to negatively impact Vis channels most strongly, as well as having some impact in the UV and TIR. Natraj et al. (2011) report multiple cases for each instrument, based on assumed atmospheric conditions. We select from their work a high sensitivity case and a low sensitivity case to characterize the range of instrument performance and provide upper and lower bounds on the information obtainable from geostationary observation. Sensitivity increases with higher thermal contrast between the surface and the atmosphere, higher boundary layer ozone concentration, higher surface albedo, and lower effective solar zenith angle.

Figure 2.1 shows the rows of the averaging kernel matrices for the high sensitivity and low-sensitivity cases weighted by level thickness. Also shown are the degrees of freedom for

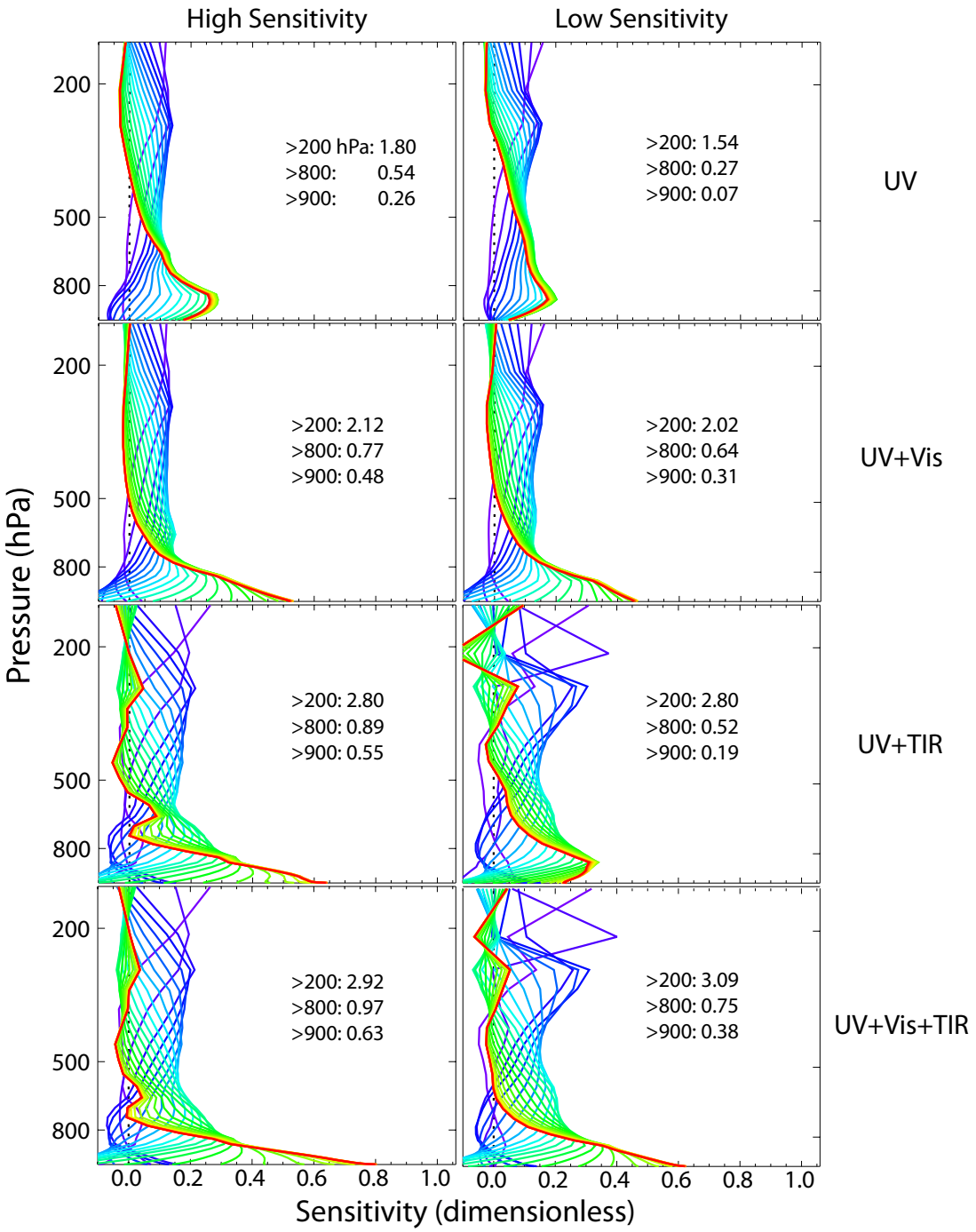

Figure 2.1: Rows of typical averaging kernel matrices for theoretical retrievals of ozone vertical profiles from geostationary ozone instruments in different spectral combinations: UV, UV+Vis, UV+TIR, and UV+Vis+TIR (Natraj et al., 2011). The color gradient from red to blue corresponds to retrievals at different levels from surface air (red) to 200 hPa (blue). Results from a high-sensitivity case (left) and a low-sensitivity case (right) are shown. Inset are the degrees of freedom for signal (DOFS) for the atmospheric columns below 200, 800, and 900 hPa.

signal (DOFS) below given pressure levels. These are as given by Natraj et al. (2011). Each line (row) gives the vertical sensitivity of the ozone retrieval at a given level to the "true" profile. The DOFS are the number of independent pieces of information in the vertical provided by the retrieval, as determined from the trace of the averaging kernel matrix. Sensitivity of UV retrievals in the boundary layer is limited by air molecular scattering (0.27-0.54 DOFS below 800 hPa). When combined with UV, the Chappuis band adds information near the surface (0.64-0.77 DOFS below 800 hPa). In the Chappuis band there is reduced molecular scattering and ozone absorption is optically thin, resulting in better transmission and an increased signal from the boundary layer. Both the UV and the UV+Vis retrievals provide more information in the high sensitivity case than in the low sensitivity case due to greater ozone concentrations in the boundary layer, higher surface albedo, and better viewing geometry. Retrievals in the TIR depend on the temperature contrast between the atmosphere and the surface as well as ozone concentration. Temperature contrast gives profile information in the upper troposphere, reflected in the peaks in the rows of the averaging kernels above 500 hPa for combinations including the TIR. In the high sensitivity case there is a strong thermal contrast between the surface radiant (skin) temperature and the air temperature, resulting in increased boundary layer information from including the TIR (0.89 DOFS below 800 hPa). This enhancement is not as strong in the low sensitivity case (0.52 DOFS below 800 hPa). For both cases the full UV+Vis+TIR combination provides the maximum information (0.75-0.95 DOFS below 800 hPa).

We used the adjoint of the GEOS-Chem ozone simulation (Henze et al., 2007; Zhang et al., 2009) to examine whether satellite information on ozone in the free troposphere would help constrain surface ozone through the forward propagation of information in the model by

atmospheric transport. **Figure 2.2** illustrates the average sensitivity of surface ozone in eastern Massachusetts and southern California to ozone production at different altitudes for two weeks in July 2006. Most of the ozone in surface air is produced below 2 km altitude, although the sensitivity to the free troposphere is stronger over southern California.

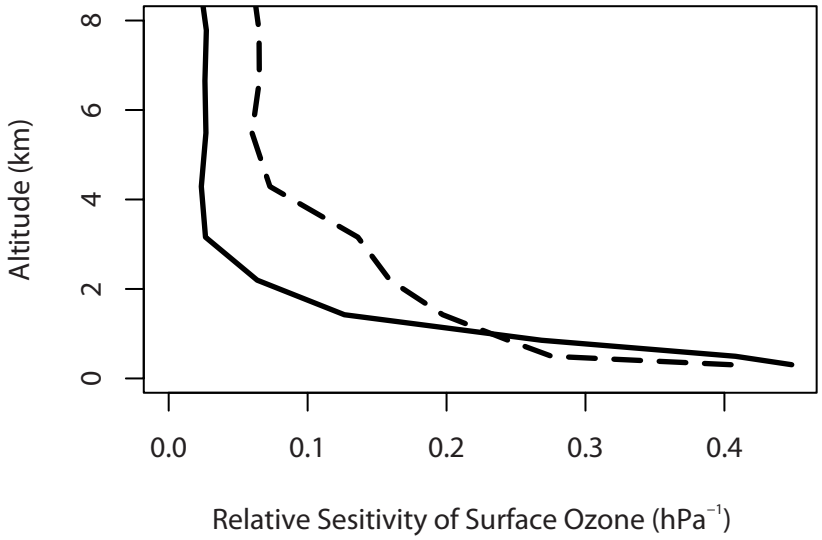

Figure 2.2: Sensitivity of surface ozone over eastern Massachusetts (42^{o} N, 72^{o} W, solid) and southern California (34^{o} N, 118^{o} W, dashed) to integrated ozone production at different altitudes, as computed from the GEOS-Chem adjoint model for 1-14 July 2006.

We conclude that the GEO-CAPE instrument requires direct boundary layer sensitivity to constrain surface ozone. Our result is consistent with a CTM tracer study in support of the Infrared Atmospheric Sounding Interferometer (IASI) by Foret et al. (2009) which showed that on average only 7% of ozone at 800 – 700 hPa over Europe reaches the surface. Parrington et al. (2009) found that assimilation of TES free tropospheric ozone into GEOS-Chem affected the simulation of boundary layer ozone by 0-9 ppbv but did not systematically improve it.

2.3 OSSE Framework

Our OSSE uses the MOZART CTM to represent the "true" atmosphere and the

GEOS-Chem CTM as the forward model, both simulating the month of July 2001. Synthetic observations of the "true" atmosphere are made for different instrument configurations using the clear sky averaging kernel matrices of **Figure 2.1**. Comparing the model states without assimilation (*a priori*) and with assimilation (*a posteriori*) to the concentrations from the "true" atmosphere measures the information retrieved from the instrument configuration.

The GEOS-Chem simulation (v8-01-01) was previously described by Wang et al. (2009) in a study of Canadian and Mexican influences on US ozone air quality. It is driven by GEOS-3 assimilated meteorological data from the NASA Global Modeling and Assimilation Office (GMAO) with 6-hour temporal resolution. It includes a full representation of tropospheric ozone-NO_x-VOC-aerosol chemistry over a nested North America domain with 1^ox1^o horizontal resolution (10^oN – 60^oN, 140^oW – 40^oW), nested within a global domain with 4^ox5^o horizontal resolution. It has 47 vertical levels, including 14 levels below 2 km and 29 levels below 10 km. It uses the Synoz flux boundary condition for the ozone source from the stratosphere (McLinden et al. 2000) For the purpose of the OSSE, ozone concentrations above the tropopause are replaced with MOZART values as described below.

For our "true" state we use hourly archived data from the MOZART-2 CTM (Fiore et al., 2011) driven by assimilated meteorological data from the National Center for Environmental Prediction (NCEP) with 1.8^ox1.8^o horizontal resolution and 28 vertical levels (8 below 2 km, 17 below 10 km). This version of MOZART uses a modified version of the Synoz flux boundary condition for the ozone source from the stratosphere. The data are horizontally averaged on the 1^ox1^o GEOS-Chem model grid. MOZART has a separate

development heritage from GEOS-Chem and uses different driving meteorological fields, chemical mechanisms, and emission inventories. There is little commonality in any aspect of the tropospheric models, which is an important attribute for our OSSE study. The coarse horizontal resolution of MOZART means that our OSSE cannot test the ability of GEO-CAPE to constrain urban-scale features and mesoscale transport of ozone. However, our focus here is on vertical sensitivity.

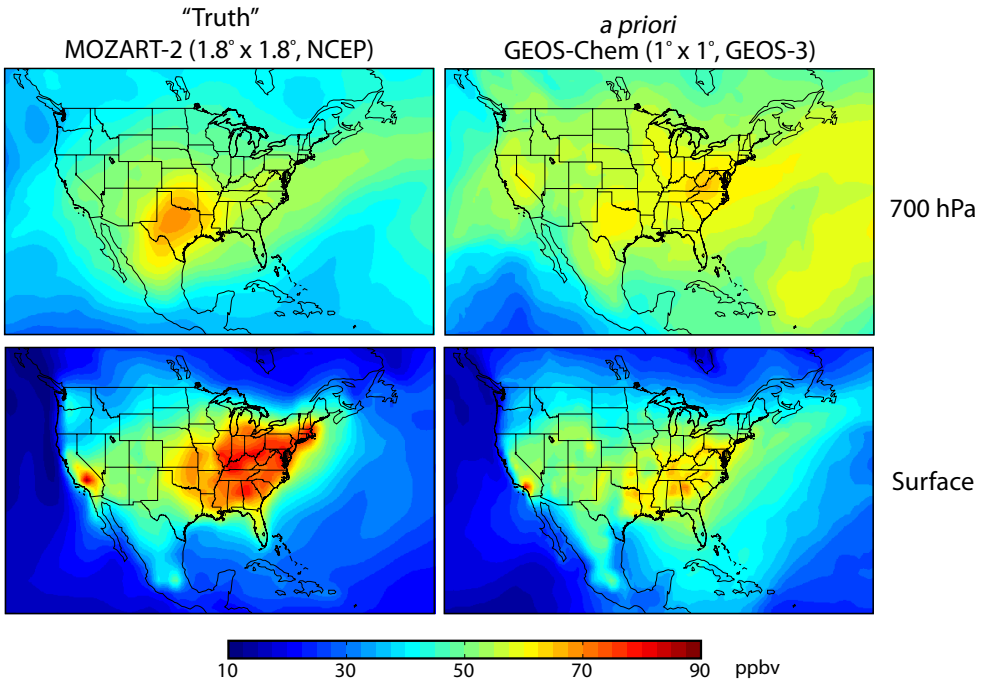

Figure 2.3: Mean 8-hour daily maximum ozone concentrations for July 2001 at 700 hPa and in surface air. Left panels show values from the MOZART CTM used as the "true" atmosphere in our OSSE. Right panels show the *a priori* values from the GEOS-Chem CTM.

Figure 2.3 shows the maximum daily 8-hour average (MDA8) ozone concentrations in the lower free troposphere (700 hPa) and in surface air for each model for July 2001. GEOS-Chem is higher than MOZART in the free troposphere over most of the domain. At the surface the patterns tends to reverse, with MOZART higher than GEOS-Chem over much of the US Northeast and Midwest. Thus the vertical gradients of ozone differ

greatly between the two models, presenting the OSSE with a challenging test. Gradient reversals between the free troposphere and the surface are consistent with our results in Figure 2 showing boundary layer ozone to be primarily constrained by production below 2 km.

We generate synthetic geostationary observations from the MOZART "true" atmosphere by sampling the hourly daytime vertical profiles over the whole domain with the averaging kernel matrices given in **Figure 2.1**. We do not sample at night, as UV+Vis observations are not available and TIR observations have less information than in daytime. We also omit scenes with cloud fraction > 0.3 (as given by the GEOS-3 meteorology). Gaussian random error is added to the synthetic observations to simulate spectral measurement error (instrument noise ε in eq. (1)) as given by Natraj et al. (2011). As the GEO-CAPE footprint (~8 km) is much finer than the GEOS-Chem resolution (~100 km), the instrument error is reduced by the square root of the number of observations available for the corresponding GEOS-Chem grid square. In the OSSE framework we assimilate the synthetic observations of the "true" state into the forward model, as we would do with actual data, to correct the mismatch between the "true" and *a priori* states. We do this sequentially by using a Kalman filter following Khattatov et al. (2000). A Kalman filter provides the best estimate of the state at a given time step using measurements at that time step and *a priori* information from previous time steps of the model (Rodgers 2000). We apply the filter iteratively at successive observation time steps to update the model state.

At an observation time step *t* we combine the local synthetic observed ozone profile $\mathbf{x'_t}$ (from eq. 1) with the model ozone profile $\mathbf{x_{at}}$ to find the *a posteriori* ozone concentration $\hat{\mathbf{x}}_t$:

$$\hat{\mathbf{x}}_t = \mathbf{x}_{at} + \mathbf{G}_t(\mathbf{x'}_t - \mathbf{K}_t\mathbf{x}_{at}) \quad (2.2)$$

where $\mathbf{K}_t$ is the observation operator at time step *t* which maps the true state to the observed state. This represents the measurement process and in our case is the instrument averaging kernel matrix, assumed to be invariant ($\mathbf{K_t = A}$). $\mathbf{G_t}$ is the Kalman gain matrix given by:

$$\mathbf{G_t} = \mathbf{S_{at}K^T}(\mathbf{KS_{at}K^T} + \mathbf{S}_\varepsilon)^{-1} \quad (2.3)$$

The gain matrix determines the relative weight given to the observations and the model. It depends on the error covariance matrices for the observations $\mathbf{S_\varepsilon} = [\boldsymbol{\varepsilon\varepsilon}^T]$ and for the model $\mathbf{S_{at}}$. Above the tropopause we replace the GEOS-Chem simulated profiles with the synthetic retrievals so that the innovation term $\mathbf{x'}_t - \mathbf{K}_t\mathbf{x}_{at}$ is solely determined by the tropospheric simulation. We used this method in the past to avoid having stratospheric errors in GEOS-Chem affect model comparisons with satellite data for tropospheric ozone (Zhang et al., 2006).

The model error $\mathbf{S_{a0}}$ is initialized using the Relative Residual Error (RRE) method (Palmer et al. 2003, Heald et al. 2004) by comparing GEOS-Chem ozone profiles to colocated ozonesonde measurements for 2006 (Zhang et al., 2010). We find that the RRE of GEOS-Chem ozone is 25% on an annual global basis and 29% for North America in summer, with no significant vertical dependence. We use 29% to specify the initial model error variances. The spatial model error covariance is parameterized by an exponential length scale as in Khattatov et al. (2000), with a length scale of 1 km in the vertical and 100 km in the horizontal.

The model error covariance is reduced by the data assimilation at each observation time step:

$$\widehat{\mathbf{S}}_t = (\mathbf{I} - \mathbf{G}_t \mathbf{K}_t)\mathbf{S}_{at} \qquad (2.4)$$

where $\widehat{\mathbf{S}}_t$ is the updated model error covariance matrix. The diagonal terms of $\widehat{\mathbf{S}}_t$ are transported as tracers in GEOS-Chem to the next time step and are augmented by a model error variance reflecting the time-dependent divergence of the model from the true state. We quantified this time-dependent error growth in a separate test comparing MOZART and GEOS-Chem evolution of ozone concentrations, starting from identical initial tropospheric ozone fields at 0 GMT on 1 July, 2001.

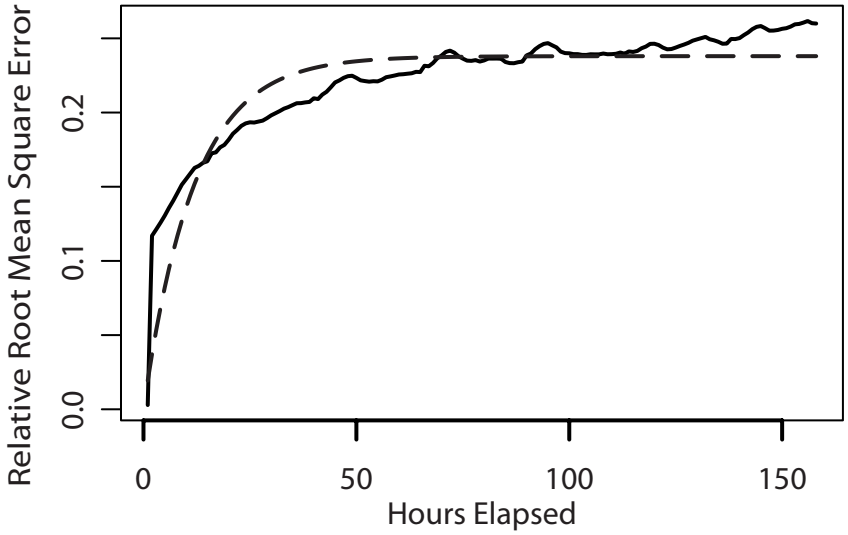

Figure 2.4: Temporal evolution of the ozone concentration error in GEOS-Chem relative to MOZART, as determined by comparing GEOS-Chem and MOZART fields in simulations with a common initialization at 0 GMT on July 1, 2001. The error statistics are measured by the relative root-mean-square error (RRMSE) for the concentration fields sampled over the North America domain. Results (solid) are fitted to an exponential function (dashed) for application to model error growth in our Kalman filter. The exponential fit gives an asymptotic error of 24% approached on a time scale of 12 hours.

Results in **Figure 2.4** show an exponential relaxation of the model relative root-mean-square error (RRMSE) with time for the simulation of ozone concentrations in the ensemble of tropospheric model grid-boxes over North America. The asymptotic RRMSE (24%) is approached on a time scale of 12 hours following initialization. The agreement between this

asymptotic value and the GEOS-Chem RRE in comparison to ozonesonde data indicates that differences between GEOS-Chem and MOZART are consistent with expected model errors relative to observations. This is an important check on the quality of the OSSE.

We checked the good behavior of our Kalman filter by comparing the mean and variance of our calculated innovation terms $\mathbf{x'}_t - \mathbf{K}_t\mathbf{x}_{at}$ to theoretical statistical predictions following Rodgers (2000). Theoretically, the innovation should be a normally distributed random variable with a mean equal to the model bias (here GEOS-Chem vs. MOZART) and a covariance equal to $\mathbf{KS}_{at}\mathbf{K}^T + \mathbf{S}_\varepsilon$. We find that this is indeed the case.

2.4 Performance of Different Instrument Configurations

Here we examine the ability of different instrument configurations and observing modes to constrain surface ozone over the US domain ($25^oN - 50^oN$, $125^oW - 65^oW$, land only). We use as our comparison metric the Root Mean Square Error (RMSE) of MDA8 ozone. The RMSE is computed only over the US, but observations are assimilated over the entire North America nested domain ($10^oN - 60^oN$, $140^oW - 40^oW$) unless otherwise specified.

We first examine the value of making observations from geostationary vs. LEO. This is done using two simulations. In the first, we assimilate observations once daily at 1300 local time (LEO). In the second, we assimilate observations once per hour during the daytime (geostationary orbit). Both simulations use the same averaging kernel matrix from the high sensitivity case for the UV+Vis+TIR instrument (**Figure 2.1**). Both are initialized on July 1 with the *a priori* GEOS-Chem ozone fields. **Figure 2.5** shows the *a priori* bias and *a posteriori* bias in MDA8 ozone averaged over July 2001 for each 1^ox1^o grid square. The *a*

priori RMSE is 8.0 ppbv ozone. The hourly observations reduce the RMSE by 54% as compared to a 19% reduction by the daily observations. We see that the hourly observations enabled by geostationary orbit allow the model to much better capture the magnitude and spatial distribution of surface ozone.

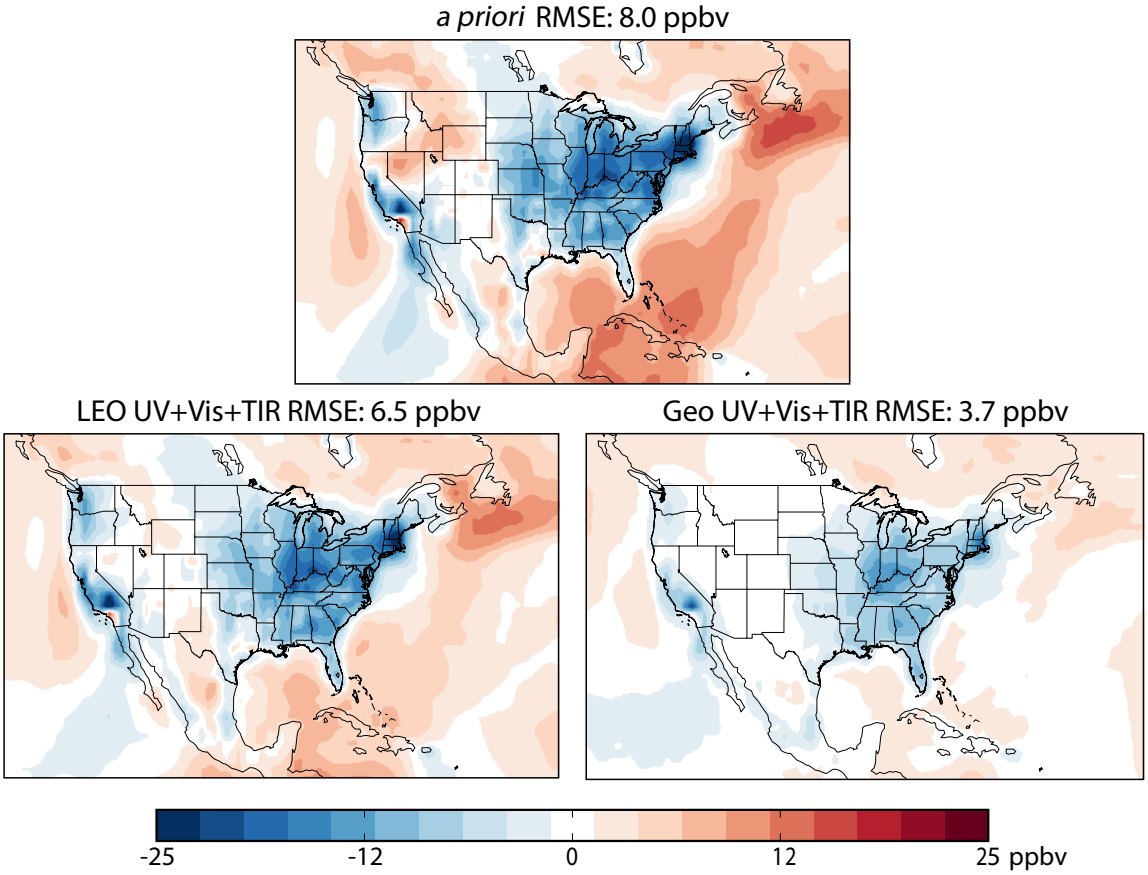

Figure 2.5: Mean bias for July 2001 in MDA8 surface ozone concentrations between the GEOS-Chem model and the MOZART model taken as the "true" atmosphere. The top panel shows the *a priori* bias before assimilation. The bottom panels show the model biases after assimilation of synthetic observations from the "true" atmosphere on a daily basis simulating a LEO instrument (left) and on a hourly basis simulating a geostationary instrument (right). The synthetic observations are for daytime only and assume a UV+Vis+TIR instrument under high-sensitivity conditions (Figure 2.1). Error statistics for the contiguous US are given as the root-mean-square error (RMSE).

One question in GEO-CAPE design is whether observing over the ocean would improve information on US air quality. In a separate simulation, we assimilate hourly

UV+Vis+TIR ozone observations as above, except with observations only over land scenes. We find that removing ocean scenes from the observing domain does not significantly impact the general ability to constrain surface ozone over the US domain (2% increase of ozone RMSE). Although there is clearly a need to extend geostationary observations some distance offshore to improve information for coastal areas (an issue that we cannot investigate at the horizontal resolution of our OSSE), we do not find a broader benefit of ocean observations for constraining US ozone air quality. Synoptic-scale recirculation of continental air masses transported offshore has occasionally been found to contribute to regional pollution episodes in the eastern US, but once these air masses are advected back over land domain they would be observed and assimilated into the model.

We now investigate the effectiveness of various spectral combinations. We simulate daytime hourly observations in the UV, UV+Vis, UV+TIR, and UV+Vis+TIR, for both the high sensitivity and low sensitivity cases. These two cases can be viewed as representing upper and lower bounds respectively for the information achievable from the observations. The spatial pattern of the correction is similar in each case to that in **Figure 2.5**, so that we use the RMSE as a single comparison statistic as described above. **Figure 2.6** shows the RMSE of MDA8 ozone over the US for all of the spectral combinations and cases simulated. In the low sensitivity case, the UV only observations (with an improved OMI-like instrument) provide a small correction, reducing the RMSE by 12% relative to the *a priori*. The full UV+Vis+TIR observations, on the other hand, remove half the *a priori* RMSE. In this low sensitivity case, adding the TIR to the UV provides less corrective power (34% reduction in RMSE) than adding the Vis (41% reduction). The relative benefit of the different combinations is different in the high sensitivity case, where thermal contrast is stronger. While the effectiveness of the

UV+Vis instrument changes little, the TIR adds much more information near the surface than it did in the low sensitivity case, reducing the RMSE by an additional 17%. In this scenario, the UV+TIR instrument is almost as successful as the UV+Vis+TIR instrument in correcting the *a priori* error.

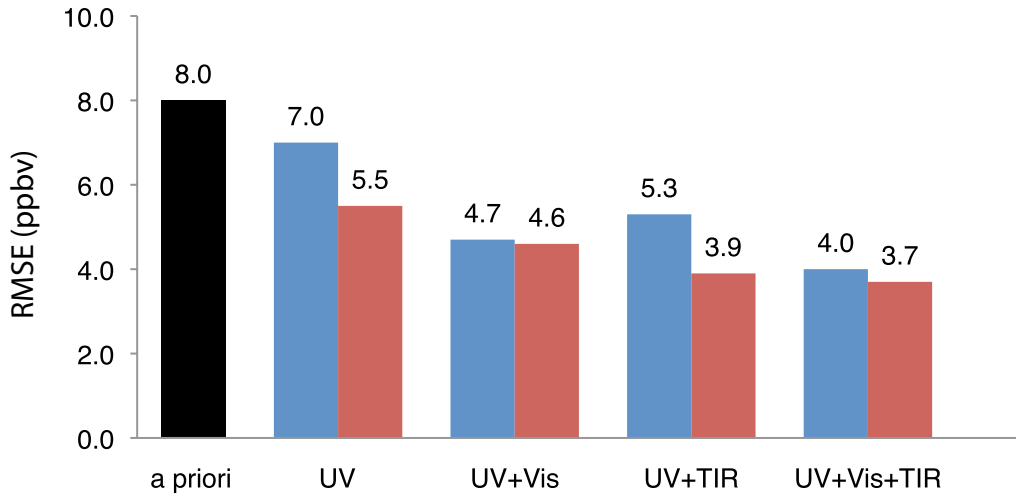

Figure 2.6: Ability of geostationary ozone measurements in different spectral combinations to constrain the ozone surface air concentration over the US. The figure shows the root-mean-square error (RMSE) of 8-hour maximum daily average (MDA8) ozone over the continental US in July 2001 relative to the "true" state defined by the MOZART model. The *a priori* error from the GEOS-Chem simulation is compared to the *a posteriori* errors after assimilation of observations from instruments in the different spectral combinations, for the high sensitivity (red) and low sensitivity (blue) cases of Figure 2.1.

A goal for the GEO-CAPE mission is to improve air quality mapping and forecasts on daily timescales. **Figure 2.7** shows a typical July timeseries of MDA8 surface ozone at Pittsburgh for the "true" state, the model *a priori*, and the model *a posteriori* with assimilated UV+Vis+IR observations from the high sensitivity case. The assimilation greatly improves the ability of the model to reproduce the daily variability in MDA8 surface ozone (*a posteriori* R^2=0.84 versus *a priori* R^2=0.52). Of particular interest is the ability of the assimilation to capture ozone exceedances of the current US air quality standard of 75 ppbv. During July, the "true" state for Pittsburgh experiences

19 days with MDA8 ozone greater than 75 ppbv. In comparison, the model *a priori* model only has 7 exceedances, while the model *a posteriori* has 13 exceedances. There are no false positives. Over the US the "true" state experiences 4,250 MDA8 ozone exceedances during July. The model *a priori* has 3,513 false negatives and 288 false positives, while the model *a posteriori* has 2,221 false negatives (37% fewer) and 49 false positives (83% fewer).

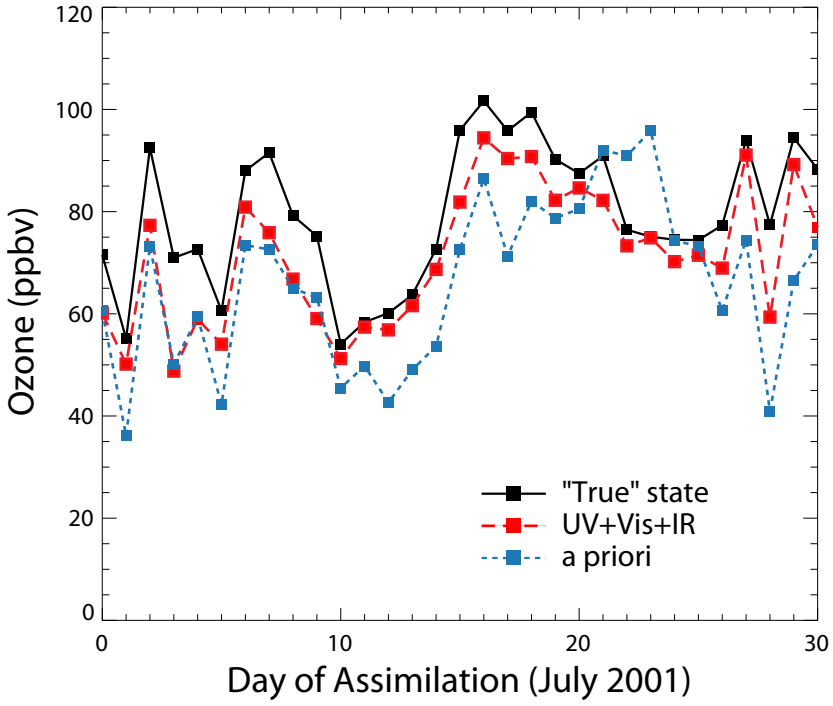

Figure 2.7: Timeseries of MDA8 surface ozone at Pittsburgh (40°N, 80°W) in July 2001 for the "true" state, the model *a priori*, and the model *a posteriori* with assimilated UV+Vis+IR observations.

Better quantifying ozone climate forcing and its relationship to sources is also a GEO-CAPE objective. This requires sensitivity to the middle and upper troposphere where ozone climate forcing is most efficient. **Figure 2.8** shows the vertical profiles of the ozone RMSE for each spectral combination, averaged over the US domain. The influence of stratospheric air is minimized by design of the OSSE (Section 3). Results are shown for the high sensitivity case:

the vertical information content is similar in the low-sensitivity case except near the surface (**Figure 2.1**). Observing in the UV alone reduces model error most efficiently in the middle troposphere between 2 and 5 km, least efficiently in the upper troposphere and near the surface. Adding Vis coverage significantly reduces the error near the surface but not at higher altitudes. Adding TIR coverage reduces the error both near the surface and in the upper troposphere, though it has little effect between 2 and 5 km. UV+Vis+TIR does not add significant information relative to UV+TIR, though we have seen previously that Vis is effective in reducing error at the surface for the low-sensitivity case.

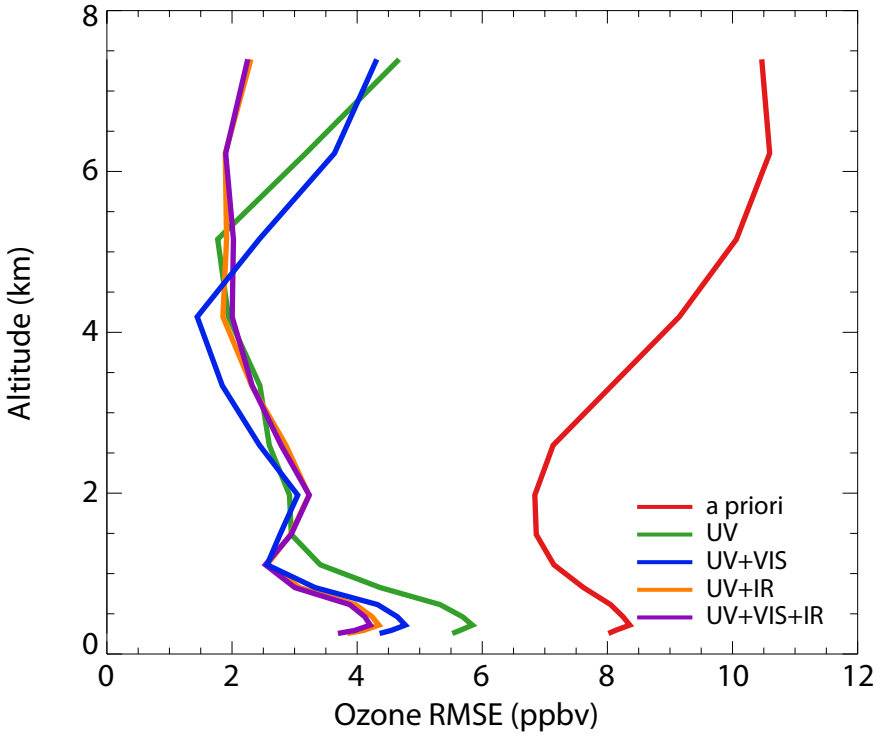

Figure 2.8: Ability of geostationary ozone measurements in different spectral combinations to constrain the vertical profile of tropospheric ozone. The figure shows the root-mean-square error (RMSE) of ozone concentrations over the continental US versus altitude in July 2001 relative to the "true" atmosphere defined by the MOZART model. The *a priori* error from the GEOS-Chem simulation is compared to the *a posteriori* errors after assimilation of observations from instruments in the different spectral combinations. Results are for the high-sensitivity case of Figure 2.1.

2.5 Summary

We conducted an observation system simulation experiment (OSSE) to determine the instrument requirements for geostationary satellite observations of ozone air quality in the US. Our aim was to inform the design of the NASA GEO-CAPE mission planned for launch by NASA in the 2020 time frame. We considered combinations of UV (Hartley-Huggins bands), Vis (Chappuis band), and TIR (9.6 μm ν_3 band) spectral regions for the candidate ozone instruments. While UV and TIR retrievals have been used before for ozone measurements from LEO, they lack sensitivity in the boundary layer which is important for air quality. The Chappuis band can provide this sensitivity. A sensitivity simulation with the adjoint of the GEOS-Chem model shows that most of the ozone in polluted areas of the US in summer is produced within the boundary layer, emphasizing the importance of sensitivity in that region.

Our OSSE framework uses 3-D hourly archives of ozone concentrations from the MOZART chemical transport model (CTM) for July 2001 as a "true" atmosphere to be sampled by the candidate instruments. We assimilate these pseudo-observations into the GEOS-Chem CTM for that month using a Kalman filter. The MOZART and GEOS-Chem CTMs have very different heritages and use different assimilated meteorological data sets, making for an objective OSSE. The error statistics between GEOS-Chem and MOZART are similar to those between GEOS-Chem and ozonesonde observations, further confirming the quality of this OSSE framework.

Our OSSE results indicate that hourly daytime observations of ozone achievable from geostationary orbit provide much better constraints on surface ozone than LEO daily observations. We also find that the geostationary observing domain can be limited to the North American continent if the measurement objective is to constrain US ozone air quality, as

observations over adjacent oceans provide little additional information. We find that multispectral observations provide much more information for surface ozone air quality than UV only. A UV+TIR combination is successful for high sensitivity conditions with strong thermal contrast at the surface, but a UV+Vis combination performs better under low sensitivity conditions. A UV+Vis+TIR combination corrects half of the *a priori* error in surface ozone. Observation in the TIR is critical to obtain ozone information in the upper troposphere relevant to climate forcing.

As part of calculating error covariance matrices for ozone data assimilation, we examined the time-dependent growth of the difference in surface air ozone concentrations simulated by GEOS-Chem and MOZART following common initialization. We find that the root-mean-square error (RMSE) between the two models reaches its asymptotic value (24%) on a time scale of only 12 hours. This means that ozone data assimilation in our OSSE environment would not enable useful air quality forecasts.

Our OSSE framework provides a general facility for addressing measurement requirements for GEO-CAPE. A limitation of the present study is the use of invariant averaging kernel matrices for the different instrument configurations. Our high sensitivity and low sensitivity cases can be viewed as providing upper and lower bounds for the information achievable from geostationary observation. We will improve in future work by using variable averaging kernel matrices responding to changes in environmental conditions. Shortcomings from using a coarse-scale "truth" model will be addressed in future work by using a regional CTM as the "truth" state. We will also examine the usefulness of complementary satellite measurements of other species (CO, NO_2, HCHO) for constraining surface ozone.

Acknowledgements

This work was supported by the NASA Atmospheric Composition and Modeling Program, by the NASA Earth Science Division, Flight Directorate, and by a NASA Earth and Space Science Fellowship to Peter Zoogman.

References:

Beer, R., 2006. TES on the Aura mission: Scientific objectives, measurements, and analysis overview. IEEE Transactions on Geoscience and Remote Sensing 44, 1102-1105.

Campbell and Fishman, 2008. NASA GEO-CAPE Workshop Report. http://geo-cape.larc.nasa.gov/docs/GEO-CAPE_Wkshp_RPt_Final-all.pdf.

Chance, K.V., Burrows, J.P., Perner, D., Schneider, W., 1997. Satellite measurements of atmospheric ozone profiles, including tropospheric ozone, from ultraviolet/visible measurements in the nadir geometry: A potential method to retrieve tropospheric ozone. Journal of Quantitative Spectroscopy & Radiative Transfer 57, 467-476.

Committee on Earth Observation Satellites, 2009. Report on the Committee on Earth Observation Satellites Atmopsheric Composition Constellation Workshop on Air Quality. http://ceos.org/images/ACC-4Reportfinal.pdf.

Edwards, D.P., Arellano, A.F., Deeter, M.N., 2009. A satellite observation system simulation experiment for carbon monoxide in the lowermost troposphere. Journal of Geophysical Research-Atmospheres 114.

Fiore, A.M., Levy, H., Jaffe, D.A., 2011. North American isoprene influence on intercontinental ozone pollution. Atmospheric Chemistry and Physics 11, 1697-1710.

Fishman, J., Bowman, K.W., Burrows, J.P., Richter, A., Chance, K.V., Edwards, D.P., Martin, R.V., Morris, G.A., Pierce, R.B., Ziemke, J.R., Al-Saadi, J.A., Creilson, J.K., Schaack, T.K., Thompson, A.M., 2008. Remote sensing of tropospheric pollution from space. Bulletin of the American Meteorological Society 89, 805-821.

Foret, G., Hamaoui, L., Schmechtig, C., Eremenko, M., Keim, C., Dufour, G., Boynard, A., Coman, A., Ung, A., Beekmann, M., 2009. Evaluating the potential of IASI ozone observations to constrain simulated surface ozone concentrations. Atmospheric Chemistry and Physics 9, 8479-8491.

Fusco, A.C., Logan, J.A., 2003. Analysis of 1970-1995 trends in tropospheric ozone at Northern Hemisphere midlatitudes with the GEOS-CHEM model. Journal of Geophysical Research-Atmospheres 108.

Heald, C.L., Jacob, D.J., Jones, D.B.A., Palmer, P.I., Logan, J.A., Streets, D.G., Sachse, G.W., Gille, J.C., Hoffman, R.N., Nehrkorn, T., 2004. Comparative inverse analysis of satellite (MOPITT) and aircraft (TRACE-P) observations to estimate Asian sources of carbon monoxide. Journal of Geophysical Research-Atmospheres 109.

Henze, D.K., Hakami, A., Seinfeld, J.H., 2007. Development of the adjoint of GEOS-Chem. Atmospheric Chemistry and Physics 7, 2413-2433.

Khattatov, B.V., Lamarque, J.F., Lyjak, L.V., Menard, R., Levelt, P., Tie, X.X., Brasseur, G.P., Gille, J.C., 2000. Assimilation of satellite observations of long-lived chemical species in global chemistry transport models. Journal of Geophysical Research-Atmospheres 105, 29135-29144.

Landgraf, J., Hasekamp, O.P., 2007. Retrieval of tropospheric ozone: The synergistic use of thermal infrared emission and ultraviolet reflectivity measurements from space. Journal of Geophysical Research-Atmospheres 112.

Lee, T.F., Nelson, C.S., Dills, P., Riishojgaard, L.P., Jones, A., Li, L., Miller, S., Flynn, L.E., Jedlovec, G., McCarty, W., Hoffman, C., McWilliams, G., 2010. NPOESS Next-Generation Operational Global Earth Observations. Bulletin of the American Meteorological Society 91, 727.

Levelt, P.F., Van den Oord, G.H.J., Dobber, M.R., Malkki, A., Visser, H., de Vries, J., Stammes, P., Lundell, J.O.V., Saari, H., 2006. The Ozone Monitoring Instrument. IEEE Transactions on Geoscience and Remote Sensing 44, 1093-1101.

Liu, X., Sioris, C.E., Chance, K., Kurosu, T.P., Newchurch, M.J., Martin, R.V., Palmer, P.I., 2005. Mapping tropospheric ozone profiles from an airborne ultraviolet-visible spectrometer. Applied Optics 44, 3312-3319.

Liu, X., Bhartia, P.K., Chance, K., Spurr, R.J.D., Kurosu, T.P., 2010. Ozone profile retrievals from the Ozone Monitoring Instrument. Atmospheric Chemistry and Physics 10, 2521-2537.

Lord, S.J., Kalnay E., Daley R., Emmitt G.D., Atlas R., 1997. Using OSSEs in the design of future generation integrated observing systems. Preprints, 1st Symposium on Integrated Observing Systems, Long Beach, CA, AMS, 45-47.

Martin, R.V., 2008. Satellite remote sensing of surface air quality. Atmospheric Environment 42, 7823-7843.

McLinden, C.A., Olsen, S.C., Hannegan, B., Wild, O., Prather, M.J., Sundet, J., 2000. Stratospheric ozone in 3-D models. Journal of Geosphysical Research 105, 14,653-14665.

Mickley, L.J., Jacob, D.J., Rind, D., 2001. Uncertainty in preindustrial abundance of tropospheric ozone: Implications for radiative forcing calculations. Journal of Geophysical Research-Atmospheres 106, 3389-3399.

Natraj, V., Liu, X., Kulawik, S., Chance, K., Chatfield, R., Edwards, D.P., Eldering, A., Francis, G., Kurosu, T., Pickering, K., Spurr, R., Worden, H., 2011. Multi-spectral sensitivity studies for the retrieval of tropospheric and lowermost tropospheric ozone from simulated clear-sky GEO-CAPE measurements. Atmospheric Environment 45, 7151-7165.

National Research Council, 2007. Earth Science and Applications from Space: National Imperatives for the Next Decade and Beyond. Washington, D.C.: National Academy Press.

Palmer, P.I., Jacob, D.J., Fiore, A.M., Martin, R.V., Chance, K., Kurosu, T.P., 2003. Mapping isoprene emissions over North America using formaldehyde column observations from space. Journal of Geophysical Research-Atmospheres, 108, 4804.

Park, R.J., Jacob, D.J., Kumar, N., Yantosca, R.M., 2006. Regional visibility statistics in the United States: Natural and transboundary pollution influences, and implications for the Regional Haze Rule. Atmospheric Environment 40, 5405-5423.

Parrington, M., Jones, D.B.A., Bowman, K.W., Horowitz, L.W., Thompson, A.M., Tarasick, D.W., Witte, J.C., 2008. Estimating the summertime tropospheric ozone distribution over North America through assimilation of observations from the Tropospheric Emission Spectrometer. Journal of Geophysical Research-Atmospheres 113.

Parrington, M., Jones, D.B.A., Bowman, K.W., Thompson, A.M., Tarasick, D.W., Merrill, J., Oltmans, S.J., Leblanc, T., Witte, J.C., Millet, D.B., 2009. Impact of the assimilation of ozone from the Tropospheric Emission Spectrometer on surface ozone across North America. Geophysical Research Letters 36.

Rodgers, C.D., 2000. Inverse methods for atmospheric sounding. River Edge, New Jersey: World Scientific.

Shindell, D.T., Faluvegi, G., 2002. An exploration of ozone changes and their radiative forcing prior to the chlorofluorocarbon era. Atmospheric Chemistry and Physics 2, 363-374.

Wang, H.Q., Jacob, D.J., Le Sager, P., Streets, D.G., Park, R.J., Gilliland, A.B., van Donkelaar, A., 2009. Surface ozone background in the United States: Canadian and Mexican pollution influences. Atmospheric Environment 43, 1310-1319.

Worden, J., Liu, X., Bowman, K., Chance, K., Beer, R., Eldering, A., Gunson, M., Worden, H., 2007. Improved tropospheric ozone profile retrievals using OMI and TES radiances. Geophysical Research Letters 34.

Worden, H.M., Bowman, K.W., Worden, J.R., Eldering, A., Beer, R., 2008. Satellite measurements of the clear-sky greenhouse effect from tropospheric ozone. Nature Geoscience 1, 305-308.

Zhang, L., Jacob, D.J., Bowman, K.W., Logan, J.A., Turquety, S., Hudman, R.C., Li, Q.B., Beer, R., Worden, H.M., Worden, J.R., Rinsland, C.P., Kulawik, S.S., Lampel, M.C., Shephard, M.W., Fisher, B.M., Eldering, A., Avery, M.A., 2006. Ozone-CO correlations determined by the TES satellite instrument in continental outflow regions. Geophysical Research Letters 33.

Zhang, L., Jacob, D.J., Kopacz, M., Henze, D.K., Singh, K., Jaffe, D.A., 2009. Intercontinental source attribution of ozone pollution at western US sites using an adjoint method. Geophysical Research Letters 36.

Zhang, L., Jacob, D.J., Liu, X., Logan, J.A., Chance, K., Eldering, A., Bojkov, B.R., 2010. Intercomparison methods for satellite measurements of atmospheric composition: application to tropospheric ozone from TES and OMI. Atmospheric Chemistry and Physics 10, 4725-4739.

Chapter 3. Improved monitoring of surface ozone air quality by joint assimilation of geostationary satellite observations of ozone and CO

[Zoogman, P., Jacob, D.J., Chance, K., Worden, H.M., Edwards, D.P., Zhang, L., Improved monitoring of surface ozone air quality by joint assimilation of geostationary satellite observations of ozone and CO, submitted to Atmospheric Environment]

Abstract

Future geostationary satellite observations of tropospheric ozone aim to improve monitoring of surface ozone air quality. However, ozone retrievals from space have limited sensitivity in the lower troposphere (boundary layer). Data assimilation in a chemical transport model can propagate the information from the satellite observations to provide useful constraints on surface ozone. This may be aided by correlated satellite observations of carbon monoxide (CO), for which boundary layer sensitivity is easier to achieve. We examine the potential of concurrent geostationary observations of ozone and CO to improve constraints on surface ozone air quality through exploitation of ozone-CO model error correlations in a joint data assimilation framework. The hypothesis is that model transport errors diagnosed for CO provide information on corresponding errors in ozone. A paired-model analysis of ozone-CO error correlations in the boundary layer over North America in summer indicates positive error correlations in continental outflow but negative regional-scale error correlations over land, the latter reflecting opposite

sensitivities of ozone and CO to boundary layer depth. Aircraft observations from the ICARTT campaign are consistent with this pattern but also indicate strong positive error correlations in fine-scale pollution plumes, We develop a joint ozone-CO data assimilation system and apply it to a regional-scale Observing System Simulation Experiment (OSSE) of the planned NASA GEO-CAPE geostationary mission over North America. We find substantial benefit from joint ozone-CO data assimilation in informing US ozone air quality if the instrument sensitivity for CO in the boundary layer is greater than that for ozone. A high-quality geostationary measurement of CO could potentially relax the requirements for boundary layer sensitivity of the ozone measurement. This is contingent on accurate characterization of ozone-CO error correlations.

3.1 Introduction

Ozone in surface air is harmful to humans and vegetation. 129 million people in the United States (US) breathe hazardous levels of ozone as measured by the National Ambient Air Quality Standard (NAAQS) of 75 ppb (maximum daily 8-hour average not to be exceeded more than 3 times per year) (US Environmental Protection Agency (EPA), 2012). Ozone is produced by photochemical oxidation of carbon monoxide (CO) and volatile organic compounds (VOCs) in the presence of nitrogen oxide radicals ($NO_x \equiv NO+NO_2$). The chemistry is complex and non-linear, making it difficult to relate ozone exceedances to precursor emissions. Satellite observations of ozone and its precursors show considerable promise for monitoring emissions and transport, as well as chemical regime (Martin 2008), but direct observation of ozone air quality from space has been limited by poor sensitivity in the boundary layer. Here we show that combined ozone and CO measurements from a geostationary satellite platform can significantly increase the observational capability for ozone through data

assimilation as compared to ozone measurements alone.

Ozone has major absorption features in the ultraviolet (UV) and the thermal infrared (TIR). These have provided the foundation for high-quality satellite retrievals of tropospheric ozone by the GOME and OMI instruments using UV solar backscatter (Liu et al., 2006, 2010) and by the TES and IASI instruments using TIR terrestrial emission (Beer, 2006; Clerbaux et al., 2009). These instruments show good consistency between themselves and with ozonesondes (Zhang et al., 2010). However, they have poor sensitivity in the lower troposphere (boundary layer), in the UV because of molecular scattering and in the TIR because of lack of thermal contrast between the surface and lowermost atmospheric air temperatures. Multispectral observation in the UV, TIR, and in the weak visible (Vis) Chappuis bands may improve sensitivity in the boundary layer in the future (Natraj et al., 2012; Fu et al., 2013; Cuesta et al., 2013). In contrast to ozone, mature CO column observations from space with boundary layer sensitivity are available from solar backscatter in the near IR (NIR), as from the SCIAMACHY instrument (Bovensmann et al., 1999). The MOPITT satellite instrument has both NIR and TIR channels, enabling separation of boundary layer and free tropospheric CO (Worden et al., 2010).

CO is a product of incomplete combustion, with an atmospheric lifetime of about two months. It is a precursor of ozone, but more importantly it is a long-lived tracer of anthropogenic influence with a mean atmospheric lifetime of about two months. Surface and aircraft observations in pollution plumes and continental outflow in summer show strong ozone-CO correlations and these have been used to test models of ozone production (Parrish et al., 1993; Chin et al., 1994; Parrish et al., 1998; Hudman et al., 2009). Concurrent TIR observations of ozone and CO from TES in the free troposphere show strong summertime correlations at northern mid-latitudes, reflecting continental outflow of ozone and intercontinental transport (Zhang et al., 2006, 2009; Hegarty et al. 2009, 2010;

Voulgarakis et al., 2011). Kim et al. (2013) combined high-density satellite data of ozone from OMI (UV) and CO from AIRS (TIR) to show patterns of strong ozone-CO correlations (positive or negative) in the free troposphere over much of the world. Negative correlations are associated with air very remote from human influence or stratospheric intrusions.

Geostationary satellite measurements of atmospheric composition promise to revolutionize our observing system for air quality over the next decade (Fishman et al., 2012). They will provide continuous hourly data with ~5 km spatial resolution over continental scales, in contrast to the current fleet of low-elevation orbit satellites that have a return time of at most once per day. We anticipate a constellation of geostationary satellites from planned launches in the 2018-2020 time frame including TEMPO over North America (http://science1.nasa.gov/missions/tempo/), SENTINEL-4 over Europe (Ingmann et al., 2012), and GEMS over East Asia (Bak et al., 2013). They will include observation of ozone in the UV (SENTINEL-4, GEMS) and UV+Vis (TEMPO). Concurrent NIR and TIR measurements of CO and ozone from co-located satellites are presently under consideration, and in the case of North America these would largely complete the atmospheric component of GEO-CAPE (Geostationary Coastal And Pollution Events) (Fishman et al., 2012), a priority strategic mission for NASA recommended by the US National Research Council Decadal Survey (2007).

Observation System Simulation Experiments (OSSEs) in support of GEO-CAPE planning have demonstrated the theoretical capability of the mission for improved observation of surface ozone (Zoogman et al, 2011) and CO (Edwards et al, 2009) through data assimilation in a chemical transport model (CTM). In data assimilation, information from the observations is used to correct the CTM (referred to as the "forward model") on the fly and with appropriate weighting of model and measurement information based on their respective uncertainties. Even though the satellite instrument does not directly measure surface air concentrations, the CTM propagates the information from the

observations to obtain an improved estimate of the 3-D concentration fields including surface values. Zoogman et al. (2011) showed that direct instrument sensitivity to the boundary layer (UV+Vis or UV+TIR channels) was necessary for GEO-CAPE to constrain surface ozone and then only with moderate success.

Here we examine whether improved estimates of surface ozone can be obtained from geostationary satellite observations through the constraint from ozone-CO error correlations in a joint assimilation of ozone and CO data. This may be particularly effective if satellite observations have more boundary layer sensitivity for CO than for ozone, as is currently the case. Diagnosed model error in simulating CO provides information on the coincident model error in simulating ozone. A similar idea has been used previously to improve CO_2 surface flux estimates through the use of combined CO_2 and CO observations together with CO_2-CO error correlations (Palmer et al., 2006; Wang et al., 2009). Statistics on ozone-CO error correlations are required, which may be different from the correlations in the concentrations themselves as pointed out by Wang et al. (2009).

Our OSSE framework involves the generation of synthetic ozone and CO data from a CTM to represent the "true" atmosphere. We use for that purpose the GEOS-Chem CTM v8-02-03 (Bey et al., 2001; http://www.geos-chem.org) driven by GEOS-5 assimilated meteorological data from the NASA Global Modeling and Assimilation Office (GMAO). We sample this 3-D field of ozone and CO "true" concentrations following the GEO-CAPE experimental design, with expected instrument errors, to mimic the observations that GEO-CAPE will provide. We then assimilate the resulting concentrations into a different GEOS-Chem CTM simulation driven by GEOS-4 meteorological data for the same period and taken as the forward model. From there we can assess the effectiveness of the GEO-CAPE observations to correct the forward model and reproduce the "true" concentration fields through data assimilation. The GEOS-4 and GEOS-5 meteorological data differ in the underlying general

circulation model, the methodology for data assimilation, and the data assimilated (Bloom et al., 2005; Rienecker et al., 2008; Ott et al., 2009). GEOS-Chem simulations of ozone and CO driven by GEOS-4 and GEOS-5 show large differences (Liu et al., 2010, 2013; Mitovski et al., 2012), and we will illustrate this below.

3.2 Joint ozone-CO data assimilation

A CTM generates a forecast of 3-D concentration fields at a given timestep by numerical integration from the previous timestep. We can reduce the forecast error by assimilating satellite observations over that timestep. The resulting optimized 3-D field of concentrations is called the *a posteriori* state. This *a posteriori* state can then be evolved forward in time by the CTM until the next timestep, when we again assimilate observations. Data assimilation not only enables improved forecasts of concentrations by correcting the successive initial conditions but also provides an optimal estimate of the state at any given time. We use here a Kalman filter where observations at discrete timesteps are used to optimize concentrations for the corresponding times, but our error correlation method is applicable to any Bayesian data assimilation technique. Previous applications of Kalman filters for assimilating ozone in a CTM have been presented by Khattatov et al. (2000) for the stratosphere and Parrington et al. (2008) for the troposphere.

Consider a nadir satellite instrument where retrieval of vertical concentration profiles from the radiance spectra is done by optimal estimation (Rodgers, 2000). Let **x** be the true vertical profile, i.e., the vector of true concentrations on a vertical grid. The retrieved profile **x'** is related to the true state **x** by the instrument averaging kernel matrix **A**, which gives the sensitivity of **x'** to **x** ($\mathbf{A} = \partial \mathbf{x}' / \partial \mathbf{x}$):

$$\mathbf{x}' = \mathbf{x}_S + \mathbf{A}(\mathbf{x} - \mathbf{x}_S) + \boldsymbol{\varepsilon} \tag{3.1}$$

where $\boldsymbol{\varepsilon}$ is the instrument noise vector and $\mathbf{x}_S$ is an independent *a priori* ozone profile used in the satellite retrieval process to constrain the solution.

In a single-species ozone assimilation we calculate an optimal *a posteriori* estimate $\hat{\mathbf{x}}$ of the ozone concentration at each observation time step as an error-weighted average of the CTM forecast $\mathbf{x}_a$ (with error vector $\boldsymbol{\varepsilon}_a$ relative to the true profile) and the observations $\mathbf{x}'$. The errors are characterized by error covariance matrices $\mathbf{S_a} = E[\boldsymbol{\varepsilon}_\mathbf{a}\boldsymbol{\varepsilon}_\mathbf{a}^T]$ and $\mathbf{S}_\boldsymbol{\varepsilon} = E[\boldsymbol{\varepsilon}\boldsymbol{\varepsilon}^T]$, where $E[\ ]$ is the expected-value operator. Assuming unbiased Gaussian distributions for $\boldsymbol{\varepsilon}_\mathbf{a}$ and $\boldsymbol{\varepsilon}$ yields an analytical least-squares solution (Rodgers, 2000)

$$\hat{\mathbf{x}} = \mathbf{x}_a + \mathbf{G}(\mathbf{x}' - \mathbf{K}\mathbf{x}_a). \tag{3.2}$$

where $\mathbf{K}$ is the observation operator that maps the state vector to the observation vector, including the vertical smoothing from the satellite retrieval and the interpolation from the model grid to the observation locations. The gain matrix $\mathbf{G}$ is given by

$$\mathbf{G} = \mathbf{S}_a\mathbf{K}^T\left(\mathbf{K}\mathbf{S}_a\mathbf{K}^T + \mathbf{S}_\varepsilon\right)^{-1}. \tag{3.3}$$

and determines the relative weight given to the observations and the model. The Kalman filter correction to the forecast concentrations is based on two terms: the gain matrix, which depends on the relative error in the model and the observations; and the innovation vector $\mathbf{x}' - \mathbf{K}\mathbf{x}_a$, which describes the mismatch between the observations and the model state.

In a joint ozone-CO assimilation we optimize ozone and CO concentrations simultaneously; the state vector is the concatenation of ozone and CO vertical profiles. The

additional information from CO observations for optimizing the ozone concentrations is incorporated as covariance between model errors in ozone and CO concentrations. This covariance is described by off-diagonal terms in the model error covariance matrix $\mathbf{S_a}$, coupling the optimization of both species:

$$\mathbf{S}_a = \begin{pmatrix} \mathbf{S}_{a,O3} & E[\boldsymbol{\varepsilon}_{a,O3}\boldsymbol{\varepsilon}_{a,CO}^T] \\ E[\boldsymbol{\varepsilon}_{a,CO}\boldsymbol{\varepsilon}_{a,O3}^T] & \mathbf{S}_{a,CO} \end{pmatrix}. \quad (3.4)$$

where the subscripts O3 and CO refer to the single-species errors, and $E[\boldsymbol{\varepsilon}_{a,O3}\boldsymbol{\varepsilon}_{a,CO}^T] = E[\boldsymbol{\varepsilon}_{a,CO}\boldsymbol{\varepsilon}_{a,O3}^T]$ is the covariance of the model errors. This covariance reflects the commonality of processes driving model error in both species; we will discuss in section 3.3 its physical basis and its computation. These coupled ozone-CO terms in the model error covariance matrix lead to corresponding terms in the gain matrix, which is then applied to the combined ozone-CO innovation vector. The optimal estimate of the ozone concentrations thus depends on the observation-model mismatch in both ozone and CO.

3.3 Characterizing ozone-CO error covariances

To perform a joint ozone-CO assimilation we must first derive the model error covariance matrix terms $E[\boldsymbol{\varepsilon}_{a,O3}\boldsymbol{\varepsilon}_{a,CO}^T]$ for use in (3.4). The model error includes contributions from errors in emissions, chemistry, and transport. Relevant emission errors mainly involve NO_x (for ozone) and CO. Errors in NO_x and CO emissions are in general not correlated. Errors in chemistry are also not expected to be correlated, at least on the scale of polluted source regions where CO (with a chemical lifetime of months) can be considered inert. We therefore focus our attention on the correlation of transport errors.

To characterize the ozone-CO transport error correlation and its geographical distribution over North America we use the "paired-model" method (Wang et al., 2009) for August 2006. In the paired-model method we conduct GEOS-Chem CTM simulations of ozone and CO (2^{o}x2.5^{o} horizontal resolution) driven by different assimilated meteorological data sets, GEOS-4 and GEOS-5, for the same period. Since the GEOS-Chem CTM simulations are otherwise the same, the pair of models produce 3-D concentration fields of ozone and CO that differ only due to meteorology. The differences in concentrations are substantial, as illustrated by the monthly mean surface values in **Figure 3.1**, demonstrating the large differences between the GEOS-4 and GEOS-5 meteorological data sets. The differences in CO concentrations are 10-20%, typical of residual errors found when comparing model to observations after having optimized emissions (Heald et al., 2004; Kopacz et al., 2009).

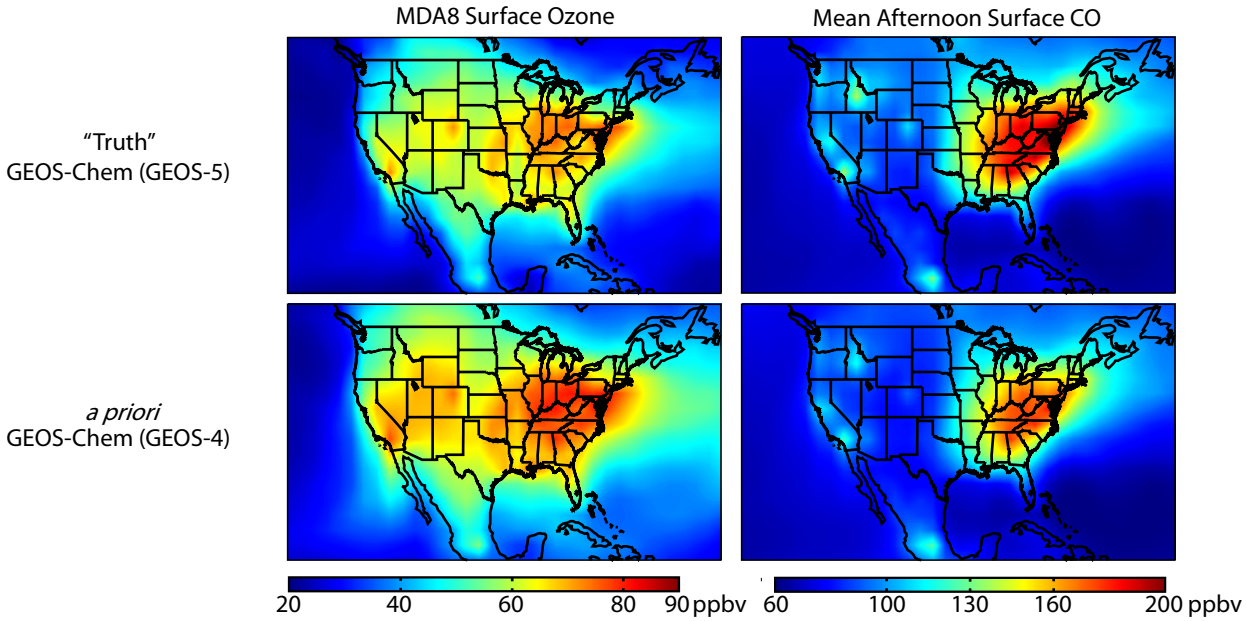

Figure 3.1: Mean values of the maximum 8-hour daily average (MDA8) ozone concentrations (left) and afternoon (1200-1700 local time) CO concentrations (right) for August 2006 in surface air. Top panels show values from the GEOS-5 model used as the "true" atmosphere in our OSSE. Bottom panels show values from the GEOS-4 model used as *a priori*.

Figure 3.2 (top) shows the ozone-CO concentration correlations in the afternoon boundary layer (0-2 km, 1200-1700 local time) in GEOS-4 for August 2006. We find a positive correlation in both GEOS-4 and GEOS-5 over most of North America and the western North Atlantic, consistent with observations (Parrish et al., 1993; Chin et al., 1994; Hudman et al., 2009). The correlation is strongest over the western North Atlantic, reflecting the contrast between North American outflow (high ozone, high CO) and clean marine air (low ozone, low CO).

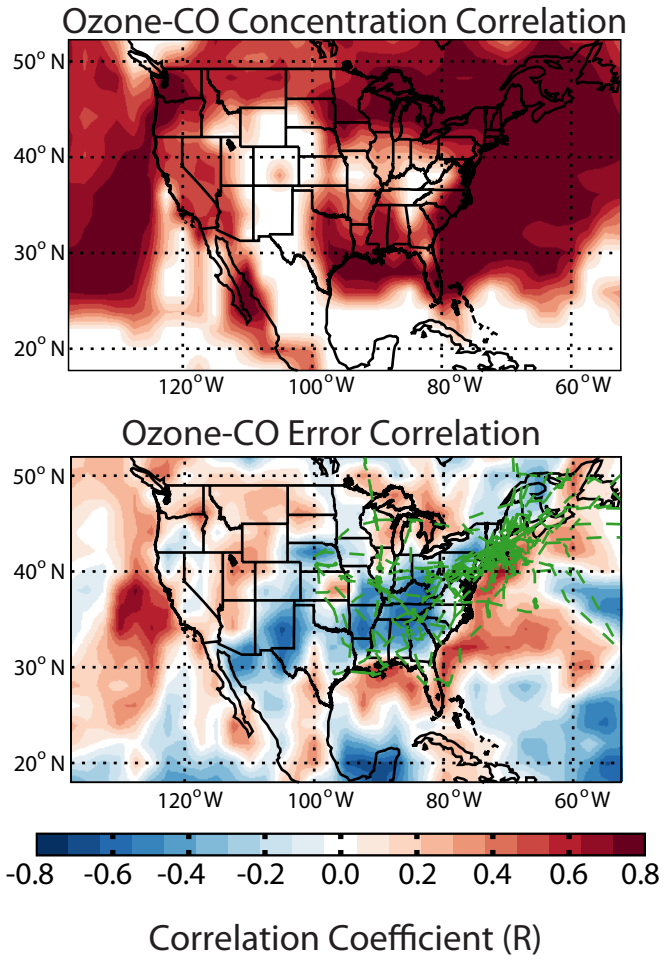

Figure 3.2: Ozone-CO concentration correlations in the afternoon boundary layer in GEOS-4 (top) and corresponding error correlations for GEOS-4 compared to GEOS-5 (bottom). Values are 0-2 km column concentrations sampled hourly at 1200-1700 local time for August 2006. Flight tracks for the ICARTT aircraft campaign are overlain (dashed green line) for comparison with Figure 3.3.

Comparison of model results for the GEOS-4 and GEOS-5 simulations in each grid square generates time series of concentration differences, Δozone and ΔCO, where Δ means "difference between GEOS-4 and GEOS-5". **Figure 3.2 (bottom)** shows the correlations between Δozone and ΔCO, the ozone-CO model error correlations. The Atlantic coastline marks a sharp boundary between negative and positive error correlations. We see that the error correlations are very different from the correlations between the concentrations themselves, as previously noted by Wang et al. (2009) for CO_2-CO. Error correlations are positive over continental outflow regions and the West but negative over the East and South. We find no significant model error correlations in the free troposphere (not shown) even though there are significant correlations in concentrations (Kim et al., 2013).

The negative ozone-CO error correlations over the East and South in **Figure 3.2** are due to differences in daytime boundary layer depths between GEOS-4 and GEOS-5. A deeper boundary layer results in more entrainment from the free troposphere, which tends to have higher ozone and lower CO concentrations than surface air (Dawson et al., 2007). Model error in boundary layer depth thus leads to anti-correlated errors in ozone and CO concentrations. In outflow regions we find a positive error correlation due to the dominant effect of horizontal transport from source regions for both ozone and CO.

Measurements from the ICARTT aircraft campaign over the eastern US and the western North Atlantic in July-August 2004 offer a test of these paired-model correlation patterns. Ozone and CO concentrations were measured from two aircraft, the NASA DC-8 and the NOAA WP-3D (Singh et al., 2006; Fehsenfeld et al., 2006). A major objective of ICARTT was to better understand ozone production in the US boundary layer and the resulting outflow (Singh et al., 2006). Hudman et al. (2009) presented a detailed analysis of ozone-CO correlations in ICARTT to address this objective.

Here we simulate the ICARTT observations using a nested continental-scale version of GEOS-Chem using GEOS-5 meteorological data with $1/2^{o}$x$2/3^{o}$ horizontal resolution (~50x50 km^2) in order to examine the correlations over different scales. The nested GEOS-Chem model is as described by Zhang et al. (2012). In all cases we sample the model along the flight tracks and at the flight times (restricted to 0-2 km, 1200-1700 local time).

Figure 3.3 (top) shows simulated and observed correlations of concentrations. Correlations are strongly positive, with consistent regression slopes (dO_3/dCO), as previously noted by Hudman et al. (2009). The model fails to reproduce concentrated pollution plumes with very high CO as these plumes are not resolved on the 50 km model scale.

The middle panel of **Figure 3.3** shows the model error (simulated – observed) in ozone concentration plotted against the corresponding model error in CO concentration for the afternoon boundary layer data. Strong positive error correlations are found in the pollution plumes (we diagnose "plumes" in the ICARTT data following Mao et al. (2013)) but the model does not resolve those as noted above. After excluding plumes, we examined the error correlations separately in the land data west of 80^{o}W and in the ocean data offshore from the eastern US, as the paired-model analysis indicates opposite correlations in these two regions (Figure 3.2). We see that the model error correlations relative to the ICARTT data are similar to those in the paired model analysis, with positive correlations over the ocean (continental outflow) and negative correlations over land (boundary layer depth). Land points east of 80^{o}W (black symbols) show positive error correlations that likely reflect a dominant influence from continental outflow. Averaging the model and observations over a 2^{o}x2.5^{o} grid (**Figure 3.3**, bottom panel) does not change the correlation statistics relative to the $1/2^{o}$x$2/3^{o}$ resolution.

Figure 3.3: Correlations between ozone and CO concentrations, and corresponding model error correlations, for afternoon boundary layer data (0-2 km, 12-17 local time) from the ICARTT aircraft campaign over the eastern US and western North Atlantic during July-August 2004 (Fehsenfeld et al., 2006; Singh et al., 2006). ICARTT flight tracks are in Figure 2. The top panel shows the correlation between concentrations in the observations and in the nested GEOS-Chem model with $1/2^{o}$x$2/3^{o}$ horizontal resolution as described in the text. The observations for individual flights are averaged over the model grid and the model is sampled at the time and location of the observations. The middle panel shows the error correlation for the difference Δ between GEOS-Chem values and ICARTT observations. The bottom panel again shows the error correlation, now averaged over a 2^{o}x2.5^{o} grid. "Land" points used in correlative analyses in the middle and bottom panels are for the longitude range 100^{o}-80^{o}W sampled by ICARTT (Figure 2). Other land points sampled by ICARTT (mainly in New England) are shown in black in the middle panel and are not used in correlative analyses. Correlation coefficients (R) and slopes of the reduced major-axis regression lines (s) are shown inset.

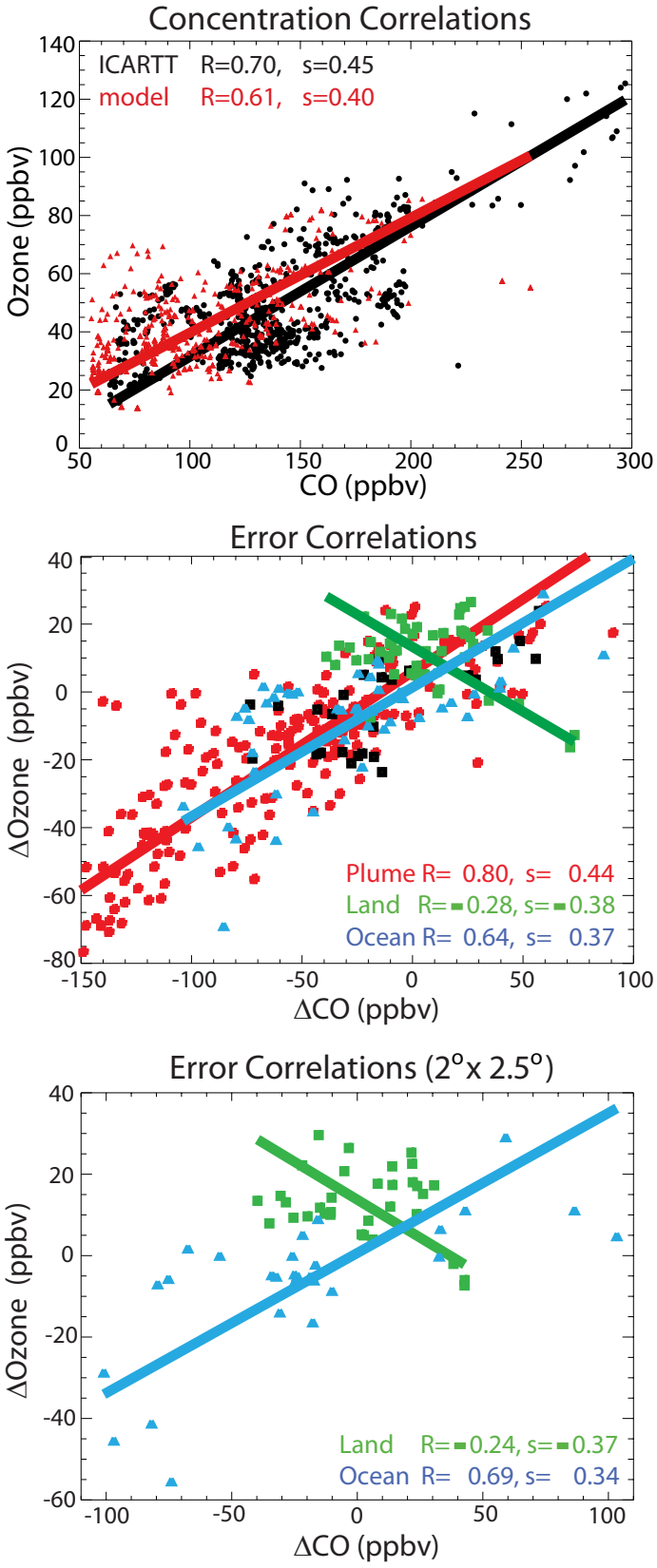

Figure 3.3 (Continued)

The switch in sign in the ozone-CO error correlation over land between pollution plumes and the 50-km model resolution has important implications. Because GEOS-Chem cannot resolve fine-scale pollution plumes, these must be excluded from the data assimilation. Such exclusion (justified by large model representation error) is standard when using atmospheric concentration data for source inversions (Palmer et al., 2003; Heald et al., 2004). Data assimilation with a finer-resolution model accounting for ozone plumes would need to use different error correlations statistics in fine-scale plumes and in regional air. The negative error correlation driven by boundary layer depth can dominate for regional air but is a minor effect for plumes relative to the positive error correlation generated by mixing the plume air (high ozone, high CO) with the cleaner background.

3.4 OSSE Design

We explore the benefit of using ozone-CO error correlations to improve data assimilation for surface ozone by performing a paired-model OSSE with GEOS-5 as the "true" atmosphere and GEOS-4 as the forward model for data assimilation, as described in Section 3. Averaging kernel matrices for the satellite instruments (**Figure 3.4**) are taken from the Natraj et al. (2011) theoretical study for GEO-CAPE ozone and from a sample NIR+TIR retrieval for MOPITT CO (Worden et al., 2010).

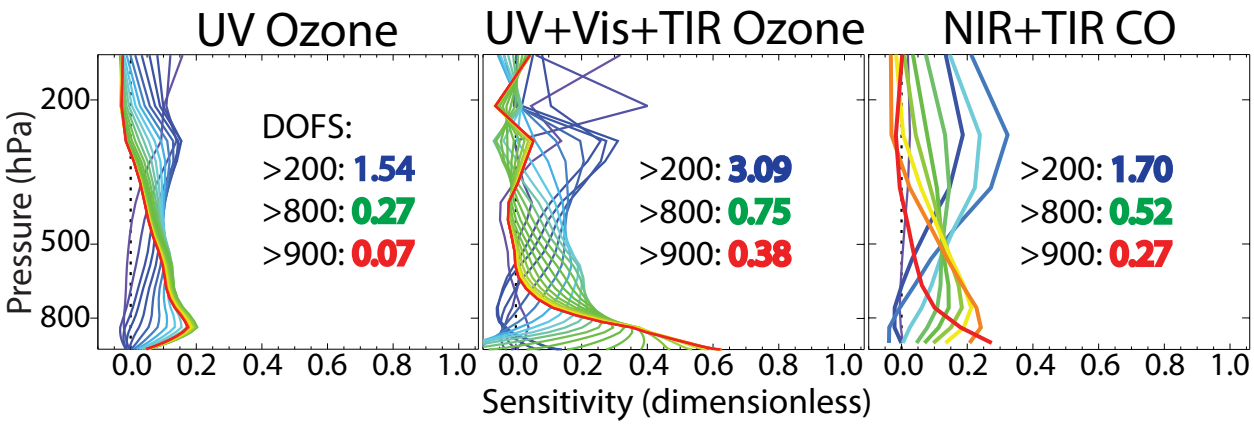

Figure 3.4: Averaging kernel matrices for clear-sky satellite retrievals of ozone and CO assumed in this study. The averaging kernel matrices are from a GEO-CAPE theoretical study by Natraj et al. [2011] for ozone in the UV and in the UV+Vis+TIR, and from a sample retrieval of CO over land by MOPITT in the NIR+TIR [Worden et al 2010]. Individual lines are the matrix rows corresponding to retrievals for individual vertical levels. The color gradient from red to blue corresponds to vertical levels ranging from the surface (red) to 200 hPa (blue). Inset are the degrees of freedom for signal (DOFS) for the atmospheric columns below 200, 800, and 900 hPa., estimated as the traces of the corresponding portions of the averaging kernel matrix.

We assume fixed averaging kernel matrices for the whole continental domain, acknowledging that there is in fact significant variability due to different surface albedos, temperatures and concentrations (Worden et al., 2013). Also shown in **Figure 3.4** are the degrees of freedom for signal (DOFS) below given pressure levels, estimated as the corresponding trace of the averaging kernel matrix and measuring the number of independent pieces of information in the retrieval (Rodgers, 2000). Sensitivity of UV ozone retrievals in the boundary layer is limited by air molecular scattering (0.27 DOFS below 800 hPa). If combined with UV, the visible and IR bands add information for near surface ozone (0.75 DOFS below 800 hPa). The multispectral NIR+TIR CO retrieval shows sensitivity to CO both near the surface (0.52 DOFS below 800 hPa) and in the free troposphere. The CO averaging kernel matrix in Figure 5 represents particularly favorable observing conditions for MOPITT, whose retrieval quality is often limited by large pixel size noise introduced by the changing view of the surface due to spacecraft motion during data scans (Deeter et al 2011). It is however

representative of the expected performance of GEO-CAPE, which will have a stationary field of regard (Fishman et al., 2012).

We generate synthetic geostationary observations from the "true" atmosphere for August 2006 by sampling the hourly daytime vertical profiles over land scenes in the North American domain with the averaging kernel matrices given in **Figure 3.4**. We omit scenes with cloud fraction > 0.3 (as given by the GEOS-5 meteorology). Gaussian random error is added to the synthetic observations to simulate spectral measurement error (instrument noise ε in eq. (3.1)) as given by Natraj et al. (2011) and Worden et al. (2010). As the GEO-CAPE footprint (~4 km) is much finer than the GEOS-Chem resolution used (~200 km), the instrument error is reduced by the square root of the number of observations available for the corresponding GEOS-Chem grid square.

We assimilate the synthetic observations of the "true" state into the forward model, as we would do with actual data, to correct the mismatch between the "true" and *a priori* states. We do this sequentially by using a Kalman filter as described in section 3.2, applying the filter iteratively at successive observation time steps to update the model state. The model error covariance matrix for each species ($\mathbf{S}_{a,O3}$ and $\mathbf{S}_{a,CO}$ in (3.4)) is assumed diagonal, and the diagonal terms are assumed constant and estimated from the Relative Residual Error (RRE) method (Palmer et al. 2003, Heald et al. 2004). This yields an altitude-independent error of 29% for ozone (Zoogman et al. 2011) and 15% for CO (Heald et al. 2004).

3.5 Error Reduction from ozone-CO Joint Assimilation

From the OSSE design in Section 3.4, we analyze the benefit of using ozone-CO model error correlations in a joint ozone-CO data assimilation system to constrain surface ozone

concentrations over the contiguous US, as compared to an ozone-only data assimilation system. We focus on the maximum daily 8-hour average (MDA8) ozone, which is the form of the national air quality standard in the US. We use two metrics to evaluate the assimilation results: (1) the Root Mean Square Error (RMSE) of MDA8 ozone relative to the "true" state, and (2) the number of incorrectly diagnosed NAAQS exceedances (MDA8 ozone >75 ppbv). These metrics are computed only over the US (25°N – 50°N, 125°W – 65°W, land only), but observations are assimilated over the entire North American domain (10°N – 60°N, 140°W – 40°W, land only). We conduct separate OSSEs for a UV-only and a UV+Vis+TIR ozone instrument, each with and without joint assimilation of CO, for a total of four OSSEs. Metrics (1) and (2) in the OSSE results are compared to the *a priori* model simulation without data assimilation.

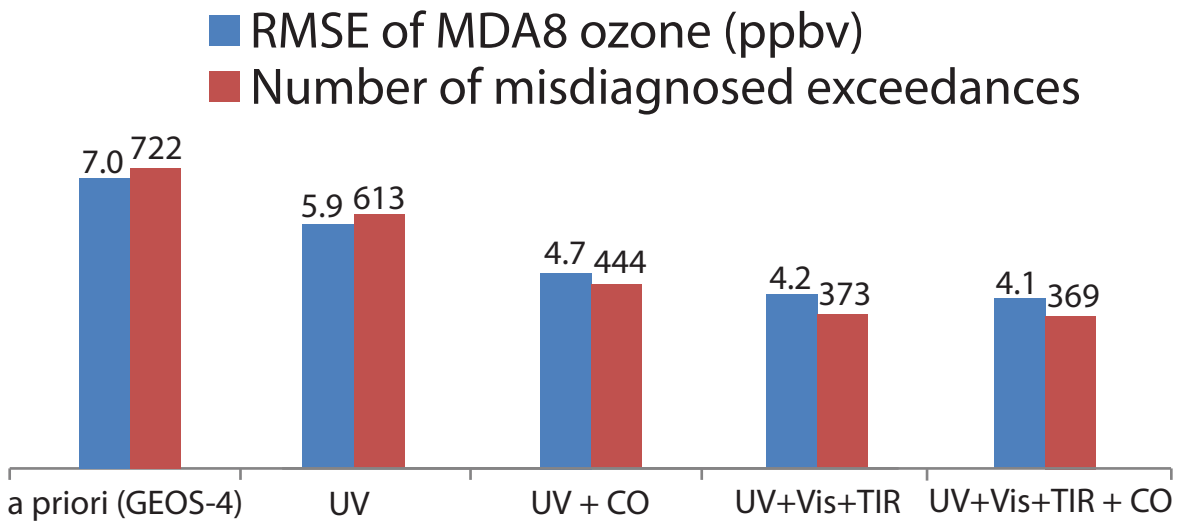

Figure 3.5: Error reduction in model simulation of surface ozone air quality from assimilation of geostationary satellite observations of ozone and CO. Results are from OSSEs for August 2006 examining two error metrics: (1) the root mean square error (RMSE) of maximum daily 8-h average (MDA8) ozone over the contiguous US relative to the "true" state defined by the GEOS-5 simulation, and (2) the number of surface gridsquare-days where the model incorrectly diagnoses a NAAQS exceedance (MDA8 ozone >75 ppbv), either as a false positive or as a false negative. The error metrics from the GEOS-4 simulation without data assimilation (*a priori*) are compared to results from the assimilation of observations from a UV-only ozone instrument (UV) and a multispectral ozone instrument (UV+Vis+TIR), without and with joint assimilation of CO using ozone-CO error correlations (+CO).

Figure 3.5 shows the data assimilation results. The RMSE for ozone without assimilation is 7.0 ppbv. For a UV-only ozone instrument, the joint ozone-CO assimilation reduces the RMSE by 33% as compared to a 16% reduction by the ozone-only assimilation. For a UV+Vis+TIR ozone instrument, the joint ozone-CO assimilation reduces the RMSE by 41% compared to a 39% reduction by the ozone-only assimilation. The CO assimilation has a major impact when the ozone instrument is UV-only, because the supplemental boundary information provided by the CO instrument is then important. The UV+Vis+TIR ozone instrument has better sensitivity to the boundary layer than the CO instrument in Figure 4, so that CO assimilation is of negligible benefit in that case. We see that joint assimilation of CO with a UV-only ozone instrument improves the representation of surface ozone concentrations in a manner that approaches the performance of the UV+Vis+TIR ozone instrument.

A goal for the GEO-CAPE mission is to improve the diagnosis and forecasting of exceedances of the ozone air quality standard. Over the US the "true" state experiences 422 gridsquare-days where MDA8 ozone exceeds 75 ppbv during August 2006. We see from **Figure 3.5** that the model *a priori* without data assimilation incurs 722 errors in diagnosing exceedances for that domain (either false positive or false negative). For a UV-only ozone instrument, the joint ozone-CO assimilation reduces the number of exceedance errors by 39%, as compared to a 15% reduction by the ozone-only assimilation. For the UV+Vis+TIR instrument, the ozone-only assimilation reduces the number of exceedance errors by 48% and the added CO assimilation has no significant benefit. These statistics and their interpretation are similar to the RMSE results.

3.6 Conclusions

We explored the value of combining geostationary satellite data for ozone and CO in a joint ozone-CO data assimilation system to inform ozone air quality. The idea is that a multispectral (NIR+TIR) CO instrument with sensitivity in the boundary layer can help to constrain surface ozone through correlation of ozone and CO errors in the chemical transport model (CTM) used for data assimilation. We implemented the joint assimilation in an Observing System Simulation Experiment (OSSE) of the planned NASA GEO-CAPE geostationary mission over North America. We considered two possibilities for the ozone instrument, UV-only or multispectral (UV+Vis+TIR).

Proper characterization of model error correlations between ozone and CO in the boundary layer is critical for the joint assimilation. These error correlations can be very different from the correlations between the concentrations themselves. We generated them by a paired-model method using GEOS-Chem CTM simulations with 2^ox2.5^o horizontal resolution driven by different assimilated meteorological data sets (GEOS-4 and GEOS-5) for the same August 2006 period. Results indicate positive ozone-CO error correlations in continental outflow regions, reflecting common horizontal transport. However, we found negative error correlations over much of the US, particularly in the Midwest (80^o – 100^o W), even though the concentrations themselves are positively correlated. These negative error correlations reflect opposite sensitivities of ozone and CO to model error in boundary layer depth.

We tested the ozone-CO error correlation patterns from the paired-model method by using ICARTT aircraft observations in the boundary layer over the eastern US and western North Atlantic during July-August 2004. Strong and consistent positive correlations are found between ozone and CO

concentrations in the observations and in a nested GEOS-Chem simulation ($1/2^{o}$x $2/3^{o}$ horizontal resolution). Error correlations between the nested GEOS-Chem simulation and the ICARTT observations are strongly positive in subgrid urban plumes and in continental outflow over the ocean, but negative over land, consistent with the paired-model statistics. GEOS-Chem is too coarse to resolve urban plumes. A fine-scale data assimilation system to resolve these plumes would need to account for the difference in error correlation between the concentrated plumes (with positive error correlation determined by common dilution of ozone and CO) and regional air (where boundary layer depth can drive a negative error correlation).

Our OSSE results indicate that adding multispectral CO measurements in a joint assimilation with UV ozone observations from geostationary orbit could provide significant improvement to constraints on surface ozone air quality. However, we find no significant benefit in the case of a multispectral UV+Vis+TIR ozone instrument with higher boundary layer sensitivity. Adding a CO measurement capability to a UV ozone observing system provides constraints on surface ozone approaching those from a UV+Vis+TIR ozone observing system, assuming that the ozone-CO error correlation statistics can be well characterized.

Our study used the same pair of models to compute the ozone-CO error correlations and to simulate the data assimilation procedure, which may overestimate the information provided by the error correlations. The OSSE would be improved through the use of a third independent model. It would obviously be best to derive the error correlations from observations, but aircraft observations are too sparse and satellite observations are smoothed by their averaging kernels. Observations can however be used to test the error correlation patterns derived from paired-model analyses, as we did here with ICARTT aircraft data.

Acknowledgements: This work was supported by the NASA Atmospheric Composition and Modeling Program and by a NASA Earth and Space Science Fellowship to Peter Zoogman.

References:

Bak, J., Kim, J.H., Liu, X., Chance, K., Kim, J., 2013. Evaluation of ozone profile and tropospheric ozone retrievals from GEMS and OMI spectra. Atmospheric Measurement Techniques 6, 239-249.

Beer, R., 2006. TES on the aura mission: Scientific objectives, measurements, and analysis overview. IEEE Transactions on Geoscience and Remote Sensing 44, 1102-1105.

Bey, I., Jacob, D., Yantosca, R., Logan, J., Field, B., Fiore, A., Li, Q., Liu, H., Mickley, L., Schultz, M., 2001. Global modeling of tropospheric chemistry with assimilated meteorology: Model description and evaluation. Journal of Geophysical Research-Atmospheres 106, 23073-23095.

Bloom, S., da Silva, A., Dee, D., Bosilovich, M., Chern, J., Pawson, S., Schubert, S., Sienkiewicz, M., Stajner, I., Tan, W., Wu, M., 2005. The Goddard Earth Observing Data Assimilation System, GEOS DAS Version 4.0.3: Documentation and Validation. NASA Tech. Rep. 104606.

Bovensmann, H., Burrows, J., Buchwitz, M., Frerick, J., Noel, S., Rozanov, V., Chance, K., Goede, A., 1999. SCIAMACHY: Mission objectives and measurement modes. Journal of the Atmospheric Sciences 56, 127-150.

Chin, M., Jacob, D., Munger, J., Parrish, D., Doddridge, B., 1994. Relationship of ozone and carbon-monoxide over north-america. Journal of Geophysical Research-Atmospheres 99, 14565-14573.

Clerbaux, C., Boynard, A., Clarisse, L., George, M., Hadji-Lazaro, J., Herbin, H., Hurtmans, D., Pommier, M., Razavi, A., Turquety, S., Wespes, C., Coheur, P., 2009. Monitoring of atmospheric composition using the thermal infrared IASI/MetOp sounder. Atmospheric Chemistry and Physics 9, 6041-6054.

Cuesta, J., Eremenko, M., Liu, X., Dufour, G., Cai, Z., Höpfner, M., von Clarmann, T., Sellitto, P., Foret, G., Gaubert, B., Beekmann, M., Orphal, J., Chance, K., Spurr, R., and Flaud, J.-M., 2013. Satellite observation of lowermost tropospheric ozone by multispectral synergism of IASI thermal infrared and GOME-2 ultraviolet measurements. Atmos. Chem. Phys. Discuss. 13, 2955-2995.

Dawson, J.P., Adams, P.J., Pandis, S.N., 2007. Sensitivity of ozone to summertime climate in the eastern USA: A modeling case study. Atmospheric Environment 41, 1494-1511.

Deeter, M.N., Worden, H.M., Gille, J.C., Edwards, D.P., Mao, D., Drummond, J.R., 2011. MOPITT multispectral CO retrievals: Origins and effects of geophysical radiance errors. Journal of Geophysical Research-Atmospheres 116, D15303.

Edwards, D.P., Arellano, A.F., Jr., Deeter, M.N., 2009. A satellite observation system simulation experiment for carbon monoxide in the lowermost troposphere. Journal of Geophysical Research-Atmospheres 114, D14304.

Fehsenfeld, F.C., Ancellet, G., Bates, T.S., Goldstein, A.H., Hardesty, R.M., Honrath, R., Law, K.S., Lewis, A.C., Leaitch, R., McKeen, S., Meagher, J., Parrish, D.D., Pszenny, A.A.P., Russell, P.B., Schlager, H., Seinfeld, J., Talbot, R., Zbinden, R., 2006. International consortium for atmospheric research on transport and transformation (ICARTT): North America to Europe - overview of the 2004 summer field study. Journal of Geophysical Research-Atmospheres 111, D23S01.

Fishman, J., Iraci, L.T., Al-Saadi, J., Chance, K., Chavez, F., Chin, M., Coble, P., Davis, C., DiGiacomo, P.M., Edwards, D., Eldering, A., Goes, J., Herman, J., Hu, C., Jacob, D.J., Jordan, C., Kawa, S.R., Key, R., Liu, X., Lohrenz, S., Mannino, A., Natraj, V., Neil, D., Neu, J., Newchurch, M., Pickering, K., Salisbury, J., Sosik, H., Subramaniam, A., Tzortziou, M., Wang, J., Wang, M., 2012. The united states' next generation of atmospheric composition and coastal ecosystem measurements NASA's geostationary coastal and air pollution events (GEO-CAPE) mission. Bulletin of the American Meteorological Society 93, 1547-+.

Fu, D., Worden, J.R., Liu, X., Kulawik, S.S., Bowman, K.W., Natraj, V., 2013. Characterization of ozone profiles derived from aura TES and OMI radiances. Atmospheric Chemistry and Physics 13, 3445-3462.

Heald, C., Jacob, D., Jones, D., Palmer, P., Logan, J., Streets, D., Sachse, G., Gille, J., Hoffman, R., Nehrkorn, T., 2004. Comparative inverse analysis of satellite (MOPITT) and aircraft (TRACE-P) observations to estimate asian sources of carbon monoxide. Journal of Geophysical Research-Atmospheres 109, D23306.

Hegarty, J., Mao, H., Talbot, R., 2010. Winter- and summertime continental influences on tropospheric O-3 and CO observed by TES over the western north atlantic ocean. Atmospheric Chemistry and Physics 10, 3723-3741.

Hegarty, J., Mao, H., Talbot, R., 2009. Synoptic influences on springtime tropospheric O-3 and CO over the north american export region observed by TES. Atmospheric Chemistry and Physics 9, 3755-3776.

Hudman, R.C., Murray, L.T., Jacob, D.J., Turquety, S., Wu, S., Millet, D.B., Avery, M., Goldstein, A.H., Holloway, J., 2009. North american influence on tropospheric ozone and the effects of recent emission reductions: Constraints from ICARTT observations. Journal of Geophysical Research-Atmospheres 114, D07302.

Ingmann, P., Veihelmann, B., Langen, J., Lamarre, D., Stark, H., Courreges-Lacoste, G.B., 2012. Requirements for the GMES atmosphere service and ESA's implementation concept: Sentinels-4/-5 and-5p. Remote Sensing of Environment 120, 58-69.

Khattatov, B., Lamarque, J., Lyjak, L., Menard, R., Levelt, P., Tie, X., Brasseur, G., Gille, J., 2000. Assimilation of satellite observations of long-lived chemical species in global chemistry transport models. Journal of Geophysical Research-Atmospheres 105, 29135-29144.

Kim, P.S., D.J. Jacob, X. Liu, J.X. Warner, K. Yang, and K. Chance, 2013. Global ozone-CO correlations from OMI and AIRS: Constraints on tropospheric ozone sources. submitted to Atmos. Chem. Phys.

Kopacz, M., Jacob, D.J., Henze, D.K., Heald, C.L., Streets, D.G., Zhang, Q., 2009. Comparison of adjoint and analytical bayesian inversion methods for constraining asian sources of carbon monoxide using satellite (MOPITT) measurements of CO columns. Journal of Geophysical Research-Atmospheres 114, D04305.

Liu, J., Logan, J.A., Murray, L.T., Pumphrey, H.C., Schwartz, M.J., Megretskaia, I.A., 2013. Transport analysis and source attribution of seasonal and interannual variability of CO in the tropical upper troposphere and lower stratosphere. Atmospheric Chemistry and Physics 13, 129-146.

Liu, J., Logan, J.A., Jones, D.B.A., Livesey, N.J., Megretskaia, I., Carouge, C., Nedelec, P., 2010. Analysis of CO in the tropical troposphere using aura satellite data and the GEOS-Chem model: Insights into transport characteristics of the GEOS meteorological products. Atmospheric Chemistry and Physics 10, 12207-12232.

Liu, X., Bhartia, P.K., Chance, K., Spurr, R.J.D., Kurosu, T.P., 2010. Ozone profile retrievals from the ozone monitoring instrument. Atmospheric Chemistry and Physics 10, 2521-2537.

Liu, X., Chance, K., Sioris, C., Kurosu, T., Spurr, R., Martin, R., Fu, T., Logan, J., Jacob, D., Palmer, P., Newchurch, M., Megretskaia, I., Chatfield, R., 2006. First directly retrieved global distribution of tropospheric column ozone from GOME: Comparison with the GEOS-Chem model. Journal of Geophysical Research-Atmospheres 111, D02308.

Mao, J., F. Paulot, D.J. Jacpb, R.C. Cohen, J.D. Crounse, P.O. Wennberg, C.A. Keller, R.C. Hudman, M.P. Barkley, and L.W. Horowitz, 2013. Ozone and organic nitrates over the eastern united states: Sensitivity to isoprene chemistry. submitted to J. Geophys. Res

Martin, R.V., 2008. Satellite remote sensing of surface air quality. Atmospheric Environment 42, 7823-7843.

Mitovski, T., Folkins, I., Martin, R.V., Cooper, M., 2012. Testing convective transport on short time scales: Comparisons with mass divergence and ozone anomaly patterns about high rain events. Journal of Geophysical Research-Atmospheres 117, D02109.

National Research Council, 2007. Earth Science and Applications from Space: National Imperatives for the Next Decade and Beyond. The National Academies Press, Washington, DC,

Natraj, V., Liu, X., Kulawik, S., Chance, K., Chatfield, R., Edwards, D.P., Eldering, A., Francis, G., Kurosu, T., Pickering, K., Spurr, R., Worden, H., 2011. Multi-spectral sensitivity studies for the retrieval of tropospheric and lowermost tropospheric ozone from simulated clear-sky GEO-CAPE measurements. Atmospheric Environment 45, 7151-7165.

Ott, L.E., Bacmeister, J., Pawson, S., Pickering, K., Stenchikov, G., Suarez, M., Huntrieser, H., Loewenstein, M., Lopez, J., Xueref-Remy, I., 2009. Analysis of convective transport and parameter sensitivity in a single column version of the goddard earth observation system, version 5, general circulation model. Journal of the Atmospheric Sciences 66, 627-646.

Palmer, P.I., Suntharalingam, P., Jones, D.B.A., Jacob, D.J., Streets, D.G., Fu, Q., Vay, S.A., Sachse, G.W., 2006. Using CO2 : CO correlations to improve inverse analyses of carbon fluxes. Journal of Geophysical Research-Atmospheres 111, D12318.

Palmer, P., Jacob, D., Fiore, A., Martin, R., Chance, K., Kurosu, T., 2003. Mapping isoprene emissions over North America using formaldehyde column observations from space. Journal of Geophysical Research-Atmospheres 108, 4180.

Parrington, M., Jones, D.B.A., Bowman, K.W., Horowitz, L.W., Thompson, A.M., Tarasick, D.W., Witte, J.C., 2008. Estimating the summertime tropospheric ozone distribution over North America through assimilation of observations from the tropospheric emission spectrometer. Journal of Geophysical Research-Atmospheres 113, D18307.

Parrish, D., Trainer, M., Holloway, J., Yee, J., Warshawsky, M., Fehsenfeld, F., Forbes, G., Moody, J., 1998. Relationships between ozone and carbon monoxide at surface sites in the North Atlantic region. Journal of Geophysical Research-Atmospheres 103, 13357-13376.

Parrish, D., Holloway, J., Trainer, M., Murphy, P., Forbes, G., Fehsenfeld, F., 1993. Export of North American ozone pollution to the north-atlantic ocean. Science 259, 1436-1439.

Rienecker, M.M., M.J. Suarez, R. Todling, J. Bacmeister, L. Takacs, H.-C. Liu, W. Gu, M. Sienkiewicz, R.D. Koster, R. Gelaro, I. Stajner, and J.E. Nielsen, 2008. The GEOS-5 Data Assimilation System—Documentation of Versions 5.0.1, 5.1.0, and 5.2.0. NASA GSFC Technical Report Series on Global Modeling and Data Assimilation, NASA/TM-2007-104606, Vol. 27, 92.

Rodgers, C.D., 2000. Inverse Methods for Atmospheric Sounding. World Scientific, River Edge, New Jersey,

Singh, H.B., Brune, W.H., Crawford, J.H., Jacob, D.J., Russell, P.B., 2006. Overview of the summer 2004 intercontinental chemical transport experiment - north america (INTEX-A). Journal of Geophysical Research-Atmospheres 111, D24S01.

United States Environmental Protection Agency, 2012. Welfare Risk and Exposure Assessment for Ozone.

Voulgarakis, A., Telford, P.J., Aghedo, A.M., Braesicke, P., Faluvegi, G., Abraham, N.L., Bowman, K.W., Pyle, J.A., Shindell, D.T., 2011. Global multi-year O-3-CO correlation patterns from models and TES satellite observations. Atmospheric Chemistry and Physics 11, 5819-5838.

Wang, H., Jacob, D.J., Kopacz, M., Jones, D.B.A., Suntharalingam, P., Fisher, J.A., Nassar, R., Pawson, S., Nielsen, J.E., 2009. Error correlation between CO2 and CO as constraint for CO2 flux inversions using satellite data. Atmospheric Chemistry and Physics 9, 7313-7323.

Worden, H.M., Deeter, M.N., Frankenberg, C., George, M., Nichitiu, F., Worden, J., Aben, I., Bowman, K.W., Clerbaux, C., Coheur, P.F., de Laat, A.T.J., Detweiler, R., Drummond, J .R., Edwards, D.P., Gille, J.C., Hurtmans, D., Luo, M., Martinez-Alonso, S., Massie, S., Pfister, G., Warner, J.X., 2013. Decadal record of satellite carbon monoxide observations. Atmospheric Chemistry and Physics 13, 837-850.

Worden, H.M., Deeter, M.N., Edwards, D.P., Gille, J.C., Drummond, J.R., Nedelec, P., 2010. Observations of near-surface carbon monoxide from space using MOPITT multispectral retrievals. Journal of Geophysical Research-Atmospheres 115, D18314.

Zhang, L., Jacob, D.J., Knipping, E.M., Kumar, N., Munger, J.W., Carouge, C.C., van Donkelaar, A., Wang, Y.X., Chen, D., 2012. Nitrogen deposition to the united states: Distribution, sources, and processes. Atmospheric Chemistry and Physics 12, 4539-4554.

Zhang, L., Jacob, D.J., Liu, X., Logan, J.A., Chance, K., Eldering, A., Bojkov, B.R., 2010. Intercomparison methods for satellite measurements of atmospheric composition: Application to tropospheric ozone from TES and OMI. Atmospheric Chemistry and Physics 10, 4725-4739.

Zhang, L., Jacob, D.J., Kopacz, M., Henze, D.K., Singh, K., Jaffe, D.A., 2009. Intercontinental source attribution of ozone pollution at western US sites using an adjoint method. Geophysical Research Letters 36, L11810.

Zhang, L., Jacob, D.J., Bowman, K.W., Logan, J.A., Turquety, S., Hudman, R.C., Li, Q., Beer, R., Worden, H.M., Worden, J.R., Rinsland, C.P., Kulawik, S.S., Lampel, M.C., Shephard, M.W., Fisher, B.M., Eldering, A., Avery, M.A., 2006. Ozone-CO correlations determined by the TES satellite instrument in continental outflow regions. Geophysical Research Letters 33, L18804.

Zoogman, P., Jacob, D.J., Chance, K., Zhang, L., Le Sager, P., Fiore, A.M., Eldering, A., Liu, X., Natraj, V., Kulawik, S.S., 2011. Ozone air quality measurement requirements for a geostationary satellite mission. Atmospheric Environment 45, 7143-7150.

Chapter 4. Monitoring high-ozone events in the US Intermountain West using TEMPO geostationary satellite observations

[Zoogman, P., Jacob, D.J., Chance, K., Liu, X., Fiore, A., Lin, M., Travis, K., in preparation for submission]

Abstract

High-ozone events, approaching or exceeding the national ambient air quality standard (NAAQS), are frequently observed in the US Intermountain West in association with subsiding background influence. Monitoring and attribution of these events is problematic because of the sparsity of the surface network and lack of vertical information. We present an Observing System Simulation Experiment (OSSE) to evaluate the ability of the future geostationary satellite instrument TEMPO (Tropospheric Emissions: Monitoring of Pollution), scheduled for launch in 2018-2019, to monitor and attribute such high-ozone events in the Intermountain West through data assimilation. TEMPO will observe ozone in the UV+Vis for sensitivity in the lower troposphere. Our OSSE uses ozone data from the AM3-Chem global chemical transport model (CTM) as the "true" atmosphere and samples it for April-June 2010 with the current surface network (CASTNet sites), TEMPO, and a low-elevation orbit (LEO) IR satellite instrument. The synthetic data are then assimilated into an independent CTM (GEOS-Chem) using a Kalman filter. Error correlation length scales (500 km in horizontal, 1.7 km in vertical) extend the range of influence of observations. We show that assimilation of surface data alone does not adequately monitor high-ozone events in the Intermountain West. Assimilation of TEMPO data greatly improves the monitoring capability, with little information added from the LEO

instrument. The vertical information from TEMPO further enables the attribution of NAAQS exceedances to background ozone and this is illustrated with the case of a stratospheric intrusion.

4.1 Introduction

Harmful impacts of surface level ozone on both humans and vegetation is of increasing concern in areas formerly considered remote. The US Environmental Protection Agency (EPA) is considering lowering the current National Ambient Air Quality Standard (NAAQS) of 75 ppbv (4^{th} highest maximum daily 8-hour average per year) to a value in the range of 60-70 ppbv (EPA, 2012). Ozone concentrations in this range are frequently observed at high-elevation sites in the western US with no local pollution influence (Lefohn et al., 2001). Although ozone levels have been decreasing over the eastern US for the past two decades due to emissions controls, there has been no such decrease in the West except for California (Cooper et al., 2012). Free tropospheric ozone at 3-8 km altitude over the western US has been increasing by 0.41 ppbv $year^{-1}$ during the past two decades (Cooper et al., 2012) and this could affect background surface concentrations in the West (Zhang et al., 2008). There has been great interest in using satellite observations of ozone and related species to monitor and attribute background surface ozone (Lin et al,. 2012a; Fu et al., 2013). This capability has been limited so far by the sparseness of satellite data and low sensitivity to the surface. All satellite measurements so far have been from low-elevation orbit (LEO). Here we show that multispectral measurements from the NASA TEMPO geostationary satellite mission over North America, scheduled for launch in 2018-2019, can provide a powerful ozone monitoring resource to complement surface sites, and can help to identify NAAQS exceedances caused by elevated background.

The North American background is defined by the EPA as the surface ozone concentration that would be present over the US in the absence of North American anthropogenic emissions. It defines the achievable benefits from domestic emissions control policies (including agreements with Canada and Mexico). The background contribution to surface ozone is particularly high in the Intermountain West, extending between the Sierra Nevada/Cascades to the west and the Rocky Mountains on the east, due to high elevation and arid terrain (Zhang et al., 2011). Subsidence of high-ozone air from the free troposphere can cause surface ozone concentrations in that region to approach or exceed the NAAQS (Reid et al., 2008). This is not an issue in the eastern US because of lower elevation, forest cover, and high moisture (Fiore et al., 2002).

Several chemical transport models (CTMs) have been used to estimate the North American background including GEOS-Chem (Fiore et al., 2003; Zhang et al., 2011), AM3-Chem (Lin et al., 2012a,b), CMAQ (Mueller and Mallard 2011), and CAMx (Emery et al., 2012). Values average 30-50 ppbv in spring and summer over the Intermountain West with events frequently exceeding 60 ppbv. However, there are large differences between models reflecting variable contributions from the stratosphere (Lin et al. 2012b), lightning (Kaynak et al. 2008, Zhang et al. 2011), and wildfires (Mueller and Mallard, 2011; Zhang et al., 2011; Jaffe and Wigder, 2012; Singh et al., 2012).

Background effects on surface ozone air quality are important to diagnose, as NAAQS exceedances can be dismissed as exceptional events if shown to be not reasonably controllable by local governances (EPA 2013). Monitoring of ozone in the Intermountain West is mostly performed at urban stations designed to observe local pollution and not background influences. There is a limited network of CASTNet sites located at national parks and other remote locations, and these have been used extensively to estimate background ozone and evaluate

models (Fiore et al., 2002; Zhang et al., 2011; Lin et al., 2012b; Cooper et al., 2012). Langford et al. (2009) demonstrated that transport of stratospheric air contributed to surface ozone in excess of 100 ppbv in Colorado in 1999. Yates et al. (2013) similarly demonstrated a stratospheric origin for a NAAQS exceedance in Wyoming in June 2012 by using a combination of 3-D modeling, aircraft observations, LEO satellite data, and geostationary weather satellites. But the current air quality observing system is very limited in its ability to (1) monitor ozone at sites prone to high background, and (2) diagnose the origin of high-ozone events at these sites.

Geostationary satellites are a promising tool to address this limitation (Fishman et al., 2012). These satellites orbit around the Earth with a 24-h period in an equatorial plane, thus continuously staring at the same scenes. Depending on the observing strategy, they may provide hourly ozone data over a continental domain, while a LEO satellite may offer at best a 1-day return time. A global constellation of geostationary satellite missions targeted at air quality is planned to launch in 2018-2019 including TEMPO (Tropospheric Emissions: Monitoring of Pollution) over North America (Chance et al. 2012), SENTINEL-4 over Europe (Ingmann et al., 2012), and GEMS over East Asia (Bak et al., 2013).

TEMPO will measure backscattered solar radiation in the 290-750 nm range, including the UV and Vis (Chappuis) ozone bands (Chance et al., 1997; Liu et al., 2005). Observation in the weak Chappuis bands takes advantage of the relative transparency of the atmosphere in the Vis to achieve sensitivity to near-surface ozone. This UV+Vis multispectral combination for ozone observation has not been used from space before. A theoretical study by Natraj et al. (2011) indicates that it should provide sensitivity to the lower troposphere. An observing system simulation experiment (OSSE) by Zoogman et al. (2011) shows that a UV+Vis instrument in geostationary orbit could provide useful constraints on surface ozone through data assimilation..

Here we conduct an OSSE to quantify the potential of geostationary ozone measurements from TEMPO to improve monitoring of ozone NAAQS exceedances in the Intermountain West and the role of background ozone in causing these exceedances. Our goal is to inform the TEMPO observing strategy and develop methods for exploitation of TEMPO data. OSSEs have previously informed mission planning for geostationary observations of atmospheric composition (Edwards et al., 2009; Zoogman et al, 2011, 2013). An important feature of our work here is the inclusion of surface network and LEO satellite observations in the data assimilation system to properly quantify the added benefit of TEMPO observations.

4.2 Observing System Simulation Experiment (OSSE)

OSSEs are a standard technique for assessing the information to be gained by data assimilation from adding a new instrument to an existing observing system (Lord et al., 1997). The OSSE framework involves the use of a CTM to generate g synthetic time-varying 3-D fields of concentrations (taken as the "true" atmosphere), and the virtual sampling of this "true" atmosphere by the different instruments composing the observing system for data assimilation. This virtual sampling follows the observing schedules and error characteristics of each instrument. The virtual observations are then assimilated in a second, independent CTM, and the results of the assimilation (with and without the new instrument) are compared to the "true" atmosphere to assess the value of the new instrument (Edwards et al., 2009).

Here we conduct an OSSE for April-June 2010, when background ozone over the Intermountain West is at its seasonal maximum (Brodin et al., 2010). The observing system includes the CASTNet surface network, a LEO instrument, and TEMPO. The "true" atmosphere is provided by the AM3-Chem CTM (Lin et al., 2012a,b). The model used for data assimilation ("forward model") is

the GEOS-Chem CTM (Zhang et al, 2011); it generates *a priori* concentrations at successive time steps to be corrected to the "true" atmosphere by the observing system through data assimilation. The information provided by the observing system is quantified by the correction of the mismatch between the "true" state and the *a priori*. We describe below our OSSE framework including the simulation models (AM3-Chem and GEOS-Chem CTMs), the observing system, and the data assimilation system.

4.2.1 Simulation Models

We use for our "true" atmosphere the global AM3-Chem CTM with horizontal resolution of $1/2^{o}$x$5/8^{o}$ (Lin et al., 2012a,b). This CTM was successful in reproducing background ozone variability and exceptional events in the Western US during the CalNex field campaign in April-June 2010 (Lin et al., 2012b). This is important because the "true" CTM should reproduce the characteristics of the observations relevant to the OSSE. Lin et al. (2012a,b) used AM3-Chem to investigate the effect of Asian transport and stratospheric intrusions on surface ozone in the Intermountain West during April-June 2010, and they quantified the ozone background through a sensitivity simulation with North American anthropogenic sources shut off. Here we use 3-hourly concentrations archived from their standard simulation to provide the global 3-D ozone fields of the "true" atmosphere.

Our forward model for data assimilation is the GEOS-Chem CTM (Bey et al., 2001; http://www.geos-chem.org) The version used here (v8-02-03) was previously described by Zhang et al. (2011) in a study of background ozone influence on the Intermountain West during 2006-2008. It covers the North America domain with $1/2^{o}$x$2/3^{o}$ horizontal resolution (10^{o}N – 60^{o}N, 140^{o}W – 40^{o}W), nested within a global domain with 2^{o}x2.5^{o} horizontal resolution. Here we apply it to April-June 2010. GEOS-Chem and AM3-Chem have completely separate development heritages

and use different driving meteorological fields, chemical mechanisms, and emission inventories. This independence between the two CTMs used in the OSSE is important for a rigorous assessment (Arnold and Dey 1986). The horizontal resolution of both CTMs (~50 km) is adequate for characterization of background ozone.

Figure 4.1 shows the maximum daily average 8-hour (MDA8) ozone concentrations in surface air for each model, averaged over April-June 2010. AM3-Chem has higher ozone concentrations than GEOS-Chem over the US as a whole and over the Intermountain West (bordered region) in particular. Zhang et al. (2011) previously showed that GEOS-Chem can reproduce ozone concentrations in the Intermountain West up to 70 ppbv with relatively little error, but cannot reproduce exceptional events of higher concentrations. AM3-Chem is biased high in the mean but better simulates high-ozone events.

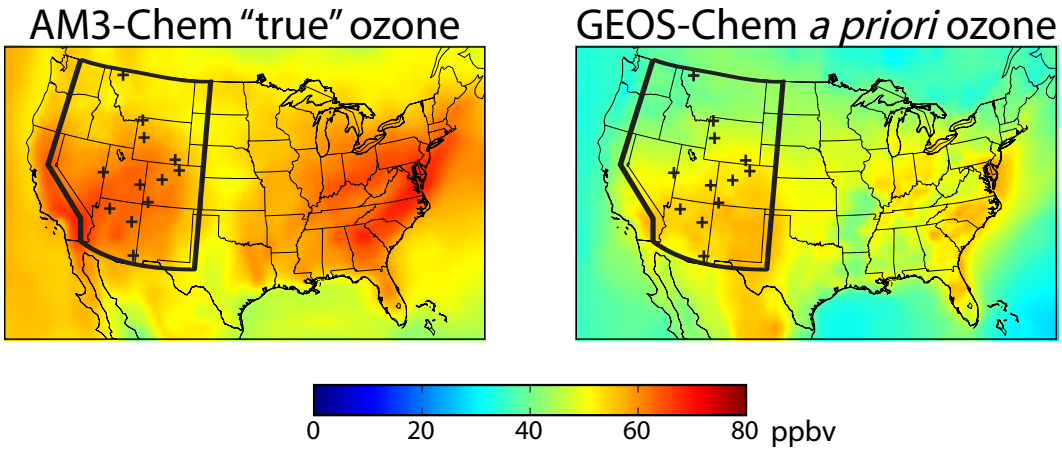

Figure 4.1: Mean values of the daily maximum 8-hour average (MDA8) ozone concentrations for April-June 2010 in surface air. Left panel shows values from the AM3-Chem CTM used as the "true" atmosphere in our OSSE. Right panel shows the *a priori* values from the GEOS-Chem CTM used for data assimilation. The black lines delineate the Intermountain West and black crosses show CASTNet surface measurement sites in the region.

4.2.2 Observing System and Synthetic Observations

Our OSSE simulates the anticipated ozone observing system over the Intermountain West during operation of TEMPO. This will consist of surface measurements, LEO satellite measurements (now becoming operational), and TEMPO geostationary satellite measurements. For the LEO satellite measurements we assume a future version of the IASI (Infrared Atmospheric Sounding Interferometer) instrument, IASI-3, that will be launched in 2016 on the MetOp-C satellite (Clerbaux, 2009). That instrument retrieves ozone in the thermal infrared (TIR). We also expect to have in that time frame UV ozone observations from the TROPOMI instrument scheduled for LEO launch in 2015 (http://www.tropomi.eu). TIR and UV ozone instruments have similar vertical sensitivities (Zhang et al., 2010). TIR has the advantage of providing observations at night that will be complementary to TEMPO.

The Clean Air Status and Trends Network (CASTNet; www.epa.gov/castnet) provides hourly data for 12 surface sites in the Intermountain West (**Figure 4.1**) that are used for background monitoring (EPA 2013). Although these sites are sparse, they are intended to be regionally representative and exhibit significant spatial correlation (Jaffe, 2011). We use these correlations in our data assimilation system as described below. CASTNet ozone measurements have 2% instrument error (EPA 2010). There is additional representation error when assimilating CASTNet data into a CTM due to the spatial mismatch between the point where the measurement is taken and the model gridsquare mean to which it is compared. We find a representation error of 5% for the ~50x50 km^2 gridsquare size of GEOS-Chem, based on the model error correlation length scale (see Section 4.2.4). During nighttime the representation error could be much larger due to surface air stratification (Fiore et al., 2002). Thus we only assimilate CASTNet data during daytime.

TEMPO and IASI-3 are both nadir viewing satellite instruments, with retrieval of vertical concentration profiles to be made by optimal estimation (Rodgers, 2000). If $\mathbf{x}_p$ is the vector of true concentrations in an observation column, the retrieved profile $\mathbf{x}_p'$ is related to $\mathbf{x}_p$ by the instrument averaging kernel matrix $\mathbf{A}$ which defines the sensitivity of $\mathbf{x}_p'$ to $\mathbf{x}_p$ ($\mathbf{A} = \partial\mathbf{x}_p'/\partial\mathbf{x}_p$):

$$\mathbf{x}_p' = \mathbf{x}_s + \mathbf{A}(\mathbf{x}_p - \mathbf{x}_s) + \boldsymbol{\varepsilon} \qquad (4.1)$$

where $\boldsymbol{\varepsilon}$ is the instrument noise vector and $\mathbf{x}_S$ is an independent *a priori* ozone profile used to regularize the retrieval.

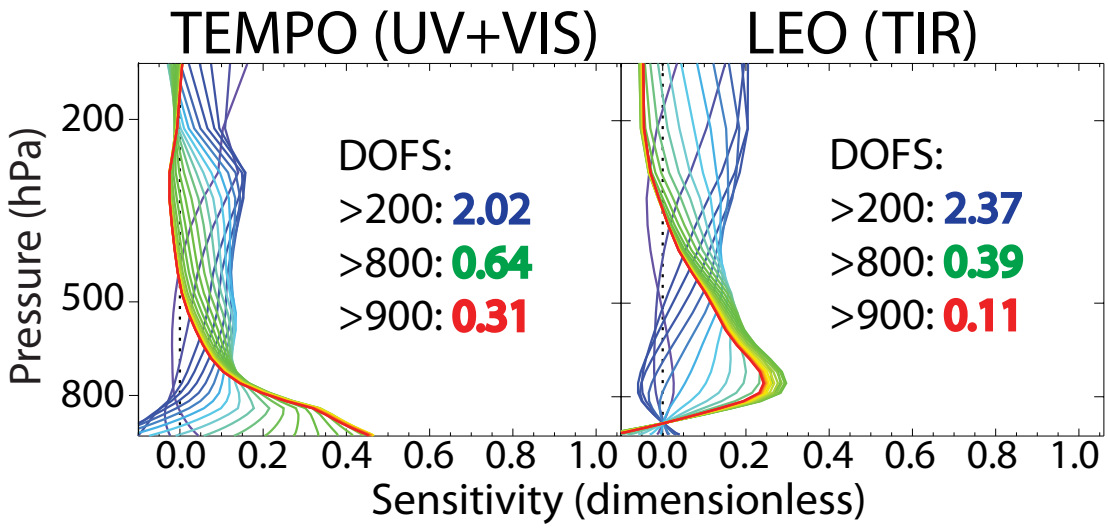

Figure 4.2: Averaging kernel matrices assumed in this study (from Natraj et al. [2011]) for clear-sky retrievals of tropospheric ozone from space in the UV+Vis (left) and the TIR (right). UV+Vis in our study corresponds to TEMPO, while TIR corresponds to a future LEO instrument flying concurrently with TEMPO. Lines are matrix rows for individual vertical levels, with the color gradient from red to blue corresponding to vertical levels ranging from surface air (red) to 200 hPa (blue). Inset are the degrees of freedom for signal (DOFS) for the atmospheric columns below 200, 800, and 900 hPa.

Figure 4.2 shows typical clear-sky averaging kernel matrices for UV+Vis and TIR retrievals of tropospheric ozone taken from the Natraj et al. (2011) theoretical study. Also shown are the degrees of freedom for signal (DOFS) below given pressure levels. The DOFS are the number of independent

pieces of information in the vertical provided by the retrieval, as determined from the corresponding trace of the averaging kernel matrix.

We generate synthetic TEMPO geostationary observations from the AM3-Chem "true" atmosphere by sampling daytime vertical profiles over land in the North American domain with the averaging kernel matrix given in **Figure 4.2**. TEMPO observations over the ocean are not included as the planned field of regard for the mission includes very little ocean and because the ocean surface is too dark for Vis retrievals. We similarly generate synthetic LEO IASI-3 observations over the North American domain (140^o-40^o W, 10^o -70^o N) twice a day (local noon and midnight) with the averaging kernel matrix given in **Figure 4.2**. We omit scenes with cloud fraction > 0.3 (as given by the GEOS meteorology). We assume fixed averaging kernel matrices, acknowledging that in practice there is significant variability (Worden et al., 2013). Gaussian noise is added to the synthetic observations following Natraj et al. (2011) to simulate the random error associated with the spectral measurement. The noise from the TEMPO instrument (footprint of 4x8 km^2) is reduced by the square root of the number of observations averaged over each GEOS-Chem grid square (~50x50 km^2) in the data assimilation process. Since the TEMPO measurements are spatially dense we assume zero representation error during assimilation. IASI measurements have footprint diameters of 12-40 km with centers spaced 25-80 km apart (August et al., 2012); no reduction of the random error is applied to the LEO observations.

4.2.3 Assimilation of surface and satellite measurements

The goal of our data assimilation system is to optimize an *n*-element state vector (**x**) of 3-D tropospheric ozone concentrations over the North American domain of GEOS-Chem, using surface and satellite observations to correct the GEOS-Chem simulation at successive time steps.

CASTNet and TEMPO data are assimilated at discrete 3-h time steps, and LEO data are assimilated at 12-h time steps. We use a Kalman filter, as previously applied to ozone data assimilation by Khattatov et al (2000), Parrington et al. (2008), and Zoogman et al. (2011). At each time step, we calculate an optimal estimate $\hat{\mathbf{x}}$ of the true ozone concentrations $\mathbf{x}$ as a weighted average of the CTM forecast $\mathbf{x}_a$ (with corresponding error vector $\boldsymbol{\varepsilon}_a$ relative to the true concentrations) and the observations $\mathbf{x}'$ (with error $\boldsymbol{\varepsilon}$, and with $\mathbf{x}'$ set to $\mathbf{x}_a$ where there are no observations). The errors are characterized by error covariance matrices $\mathbf{S}_a = E[\boldsymbol{\varepsilon}_a \boldsymbol{\varepsilon}_a^T]$ and $\mathbf{S}_\varepsilon = E[\boldsymbol{\varepsilon}\boldsymbol{\varepsilon}^T]$, where $E[\ ]$ is the expected-value operator. Assuming Gaussian error distributions for $\boldsymbol{\varepsilon}_a$ and $\boldsymbol{\varepsilon}$ we obtain (Rodgers, 2000):

$$\hat{\mathbf{x}} = \mathbf{x}_a + \mathbf{G}(\mathbf{x}' - \mathbf{K}\mathbf{x}_a) \tag{4.2}$$

where $\mathbf{K}$ is the observation operator that maps the state vector to the observation vector. For satellite measurements $\mathbf{K}\mathbf{x}_a = \mathbf{x}_s + \mathbf{A}(\mathbf{x}_a - \mathbf{x}_s)$ (equation (1) with no noise term), while for surface measurements $\mathbf{K}\mathbf{x}_a = \mathbf{x}_a$. The gain matrix $\mathbf{G}$ is given by

$$\mathbf{G} = \mathbf{S}_a \mathbf{K}^T \left(\mathbf{K}\mathbf{S}_a \mathbf{K}^T + \mathbf{S}_\varepsilon \right)^{-1} \tag{4.3}$$

and determines the relative weight given to the observations and the model. The instrument error covariance matrix $\mathbf{S}_\varepsilon$ is assumed diagonal and set to an arbitrarily large number in locations where there are no observations. For surface measurements we include the 5% representation error in quadrature with the 2% instrument error to define the instrument error covariance matrix. The optimal estimate $\hat{\mathbf{x}}$ has error $\hat{\boldsymbol{\varepsilon}}$ with error covariance $\hat{\mathbf{S}} = E[\hat{\boldsymbol{\varepsilon}}\hat{\boldsymbol{\varepsilon}}^T]$:

$$\hat{\mathbf{S}} = \left(\mathbf{I}_n - \mathbf{G}\mathbf{K} \right) \mathbf{S}_a \tag{4.4}$$

Where $\mathbf{I}_n$ is the identity matrix of dimension n.

The model error covariance matrix $\mathbf{S}_a$ expresses the error in the forward model at each assimilation time step and is given by:

$$\boldsymbol{S}_a = \begin{pmatrix} \mathrm{var}(\boldsymbol{\varepsilon}_{a,1}) & \cdots & \mathrm{cov}(\boldsymbol{\varepsilon}_{a,1}, \boldsymbol{\varepsilon}_{a,n}) \\ \vdots & \ddots & \vdots \\ \mathrm{cov}(\boldsymbol{\varepsilon}_{a,n}, \boldsymbol{\varepsilon}_{a,1}) & \cdots & \mathrm{var}(\boldsymbol{\varepsilon}_{a,n}) \end{pmatrix} \qquad (4.5)$$

where $\boldsymbol{\varepsilon}_a = (\boldsymbol{\varepsilon}_{a,1},\ldots,\boldsymbol{\varepsilon}_{a,n})^T$, with $\boldsymbol{\varepsilon}_{a,i}$ representing the error for GEOS-Chem gridbox i . At each assimilation time step the forward model error is decreased as described by the *a posteriori* error covariance matrix $\hat{\mathbf{S}}$ (equation (4.4)). The diagonal terms of $\hat{\mathbf{S}}$ are transported as tracers in GEOS-Chem to the next assimilation time step and are augmented by a model error variance reflecting the time-dependent divergence of the model from the true state following Zoogman et al. (2011). This yields the diagonal terms var($\boldsymbol{\varepsilon}_{a,i}$) of $\mathbf{S}_a$. The off-diagonal terms (error covariances) describe the propagation of information from each observation over a spatial domain of influence. We compute cov($\boldsymbol{\varepsilon}_{a,i}$, $\boldsymbol{\varepsilon}_{a,j}$) for each pair of gridboxes (*i,j)* as a function of the horizontal and vertical distance between the two gridboxes using the error correlation length scales from section 4.2.4.

In practice the dimension of the matrices used in the assimilation is limited to make the problem computationally tractable. Solution to (4.2) for each grid column is calculated ignoring satellite measurements at a horizontal distance away greater than 510 km (the horizontal error correlation length scale, see below).

4.2.4 Error Correlation Length Scales

The spatial extent of information provided by an observation to correct the GEOS-Chem model simulation through data assimilation can be quantified by correlating the GEOS-Chem errors relative to *in situ* observations at different sites in the Intermountain West (for the horizontal scale) and ozonesonde profiles (for the vertical scale) . To define a horizontal error

correlation length scale we used actual CASTNet surface measurements from our period of study (April-June 2010), downloaded from http://epa.gov/castnet/. We compute the time series of model error during daytime (0900 – 1700 LT) at each surface site, and from there derive the model error correlation between each pair of surface sites. **Figure 4.3 (left)** shows the correlation coefficients plotted against the distance *d* between sites (binned every 100km). We find R=exp(-*d*/510 km). We also show the error correlation length scale calculated when comparing the GEOS-Chem CTM and the AM3-Chem CTM (in red) sampled over the Intermountain West region. The model-model error correlation length scale is similar to the model-observation length scale and this provides some support for the realism of error patterns in our OSSE. We assume that the horizontal error correlation length scale is invariant with altitude.

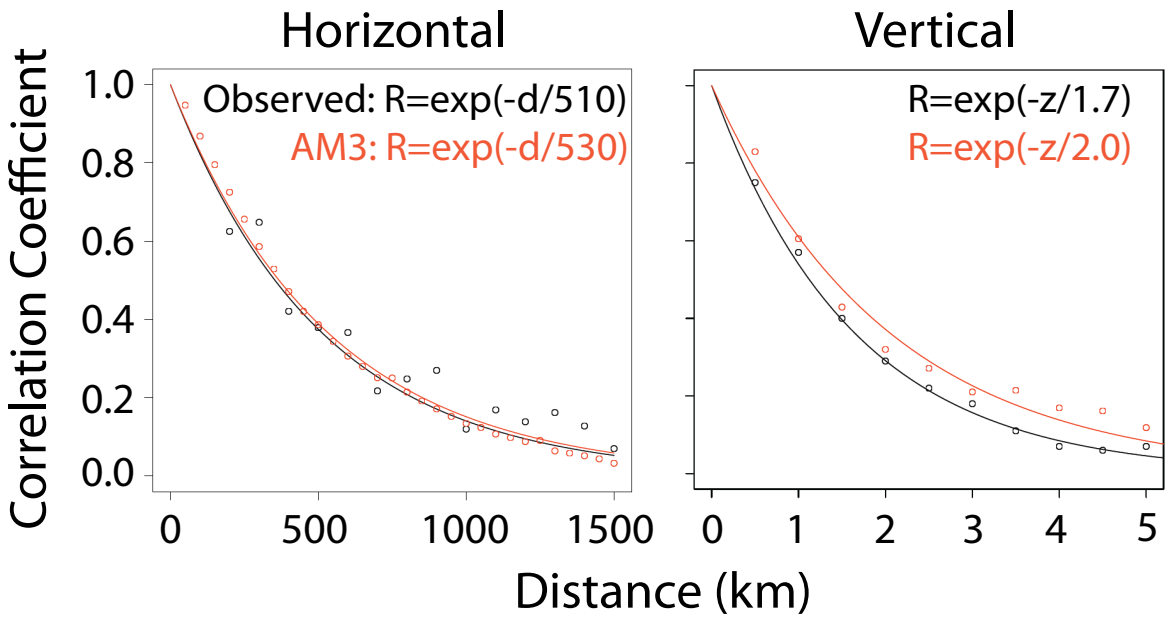

Figure 4.3: Error correlation length scales for the GEOS-Chem model simulation of tropospheric ozone in the US Intermountain West. The error correlations are relative to actual CastNet and ozonesonde observations (in black) and relative to the AM-3 model sampled in the Intermountain West region (in red). Statistics are computed for April-June 2010. The left panel shows the correlation coefficient (R) of the model error between pairs of CASTNet sites, plotted against the distance between sites. Values are for the 12 CASTNet sites in the Intermountain West (Figure 4.1). The right panel shows the correlation coefficient of the model error between pairs of vertical levels (up to 8 km altitude) for ozonesonde measurements from the IONS-2010 campaign in California [Cooper et al. 2011], plotted against distance between levels.

Exponential fits to the data are shown inset, where *d* and *z* are horizontal and vertical distances in km.

To estimate the vertical correlation length scale we compare GEOS-Chem ozone concentrations to *in situ* vertical profiles from May-June 2010 ozonesondes at six locations in California (Cooper et al. 2011). **Figure 4.3 (right)** shows the correlation coefficients plotted against the vertical distance *z* (binned every 500 m) for the time series of model errors at each ozonesonde station from the surface to 8 km altitude. We find R=exp(-*z*/1.7 km). Again, the model-model length scale (red) is not significantly different from the model-observation length scale.

4.3 TEMPO observation of high-ozone events in the Intermountain West

We now apply our data assimilation system to evaluate the benefit of TEMPO observations to monitor and attribute ozone exceedances in the Intermountain West. We compare the "true" concentrations in surface air over the Intermountain West to GEOS-Chem CTM ozone concentrations without data assimilation (*a priori*) and with assimilation of synthetic CASTNet, TEMPO, and LEO observations. We also performed an assimilation of CASTNet and TEMPO observations without a LEO instrument and found no significant difference in assimilation results. Thus the LEO instrument does not add significant information beyond TEMPO for constraining surface ozone concentrations in the Intermountain West. Its value for tracking exceptional events will be discussed in section 4.4.

Figure 4.4 examines the ability of the data assimilation system to monitor daily MDA8 ozone over the Intermountain West at the $1/2^{o}$x$2/3^{o}$ (~50x50 km^2) GEOS-Chem grid resolution. The top panel shows a scatterplot of *a priori* GEOS-Chem MDA8 ozone concentrations in April-

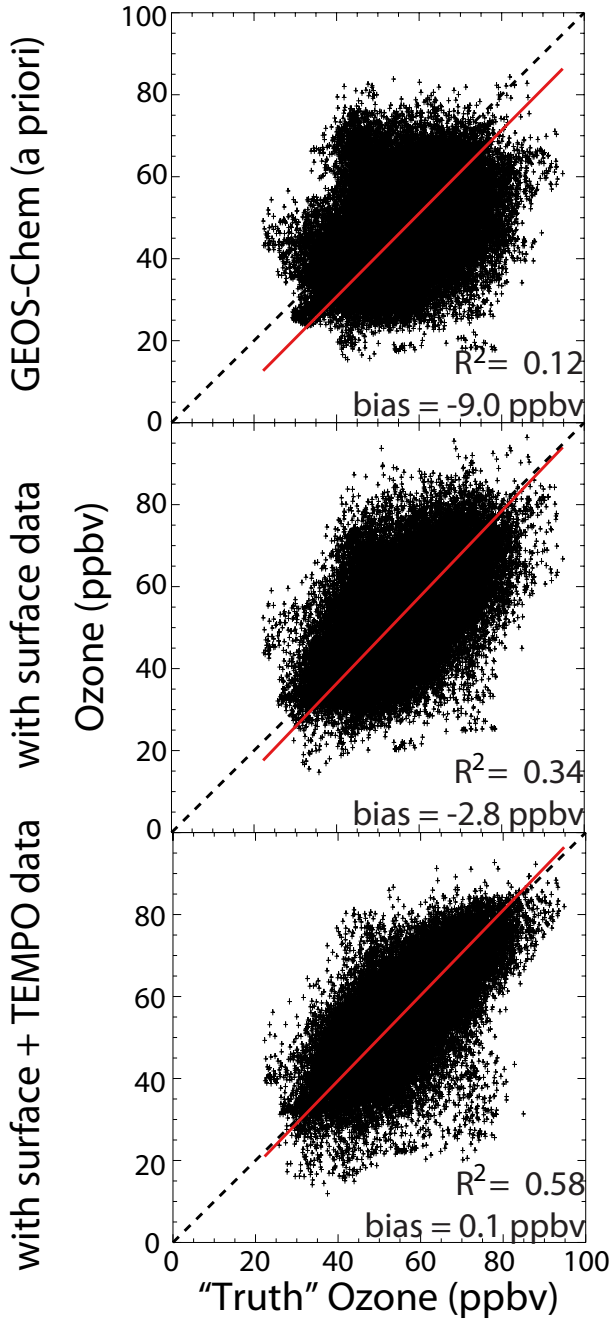

Figure 4.4: Improved monitoring of surface ozone across the Intermountain West from data assimilation of CastNet (surface) and TEMPO (geostationary satellite) observations. The figure shows scatterplots of simulated (GEOS-Chem) vs. "truth" (AM-3) daily maximum 8-h (MDA8) surface ozone for April-June 2010 for all $1/2^{o}$x$2/3^{o}$ grid squares in the region (Figure 4.1) and for individual days. Results are for GEOS-Chem without data assimilation (top), with assimilation of CASTnet synthetic surface data (middle), and with additional assimilation of TEMPO, and LEO synthetic satellite data (bottom). Comparison statistics are inset. Also shown are the reduced-major-axis (RMA) regression line and the 1:1 line.

June 2010, for individual grid squares over the Intermountain West domain of Figure 1 and individual days, vs. the "true" concentrations from the AM3-Chem model. The GEOS-Chem *a priori* is biased low and performs poorly in reproducing the "true" variability (R^2=0.12, bias = -9.0 ppbv). Assimilation of synthetic CASTNet surface measurements reduces the low bias from 9.0 to 2.8 ppbv, but still does not capture much of the variability (R^2=0.34). Adding the synthetic TEMPO geostationary observations eliminates the low bias and captures over half of the variability (R^2=0.58).

The ability of TEMPO observations to capture high-ozone events is of particular interest. **Figure 4.5** shows a map of the number of days in April-June 2010 with MDA8 ozone in excess of 70 ppbv for individual GEOS-Chem gridsquares in the Intermountain West. Values are shown for the "true" atmosphere, the GEOS-Chem *a priori* without data assimilation, and the data assimilation results including only the CASTNet observations and with the addition of TEMPO observations. The "truth" shows an average of 5.7 high-ozone events per gridsquare in the Intermountain West over the April-June 2010 period. The *a priori* model has only 0.8 event-days and the spatial pattern is very different (spatial correlation R^2=0.09 for the ensemble of Intermountain West gridsquares). Assimilation of surface measurements improves both the average number of high-ozone events (3.6 event-days) and the spatial pattern (R^2=0.62). The inability to fully correct the bias is due in part to the large impact of free tropospheric air in driving high-ozone events, and in part to the limited coverage from the sparse surface network. Adding TEMPO satellite observations almost fully corrects the bias (mean of 5.4 event-days) and captures most of the spatial distribution of high-ozone events (R^2=0.82).

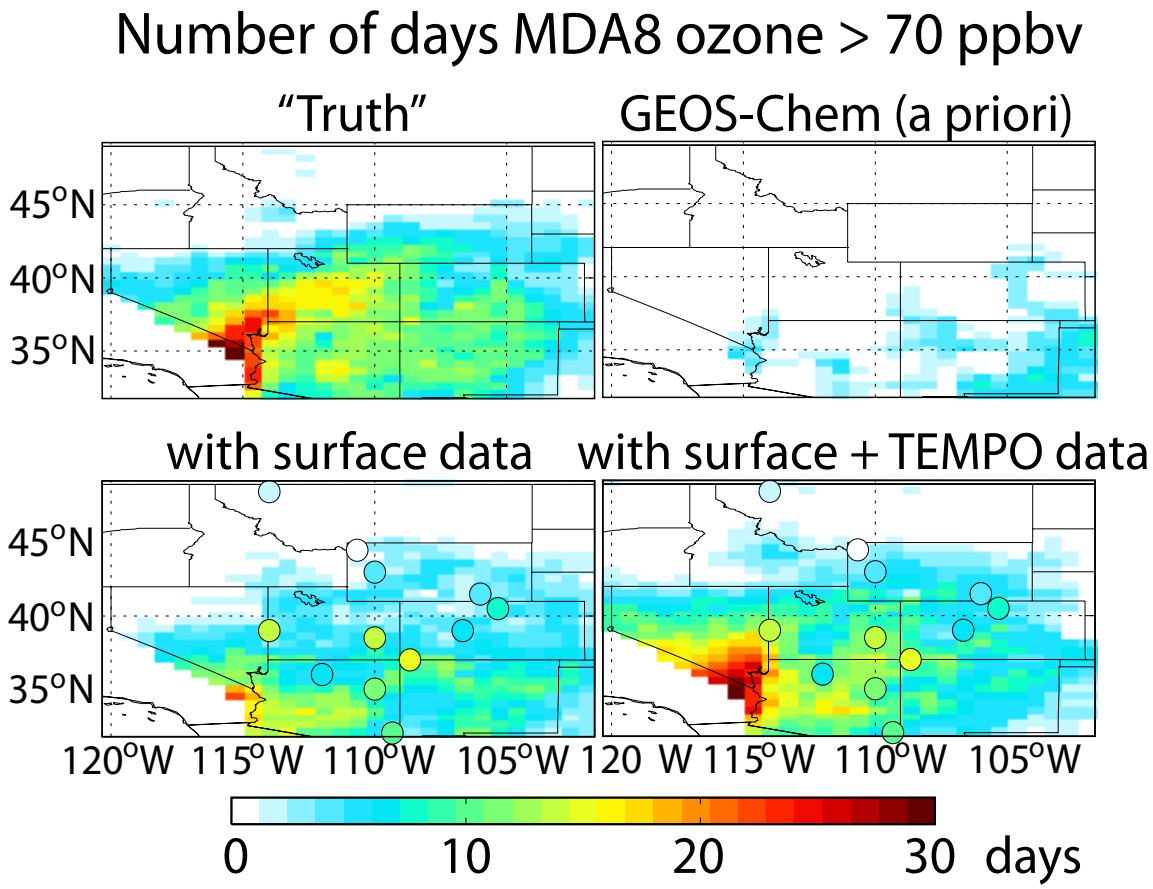

Figure 4.5: Improved detection of high-ozone events in the Intermountain West by data assimilation. The figure shows the number of events (daily maximum 8-h ozone > 70 ppbv) in April-June 2010 on the GEOS-Chem grid. The "truth" defined by the AM-3 model (top left panel) is compared to GEOS-Chem simulations without data assimilation (top right), with assimilation of CASTNet surface data (bottom left), and with additional assimilation of TEMPO and LEO satellite data (bottom right). Locations of CASTNet surface sites used for assimilation with their "true" values are overlain.

4.4 Attribution of exceptional events using TEMPO observations

TEMPO provides continuous observation in the free troposphere as well as in the boundary layer, with separation between the two (Figure 4.2). Thus it could be particularly powerful in quantifying free tropospheric background contributions to NAAQS exceedances and assist in the designation of exceptional events where an exceedance of the NAAQS is considered to be outside local control.

We examine a case study of a stratospheric intrusion on June 13 in the AM3-Chem model taken as the "truth". **Figure 4.6** shows a time series for June 2010 of MDA8 ozone concentrations at a location in northern New Mexico (107°W, 36°N). We choose this event as it was diagnosed by Lin et al. (2012b) as a major stratospheric event in the Intermountain West. Actual observations at nearby CASTNet locations indicate ozone in excess of 75 ppbv during the June 12-15 period.

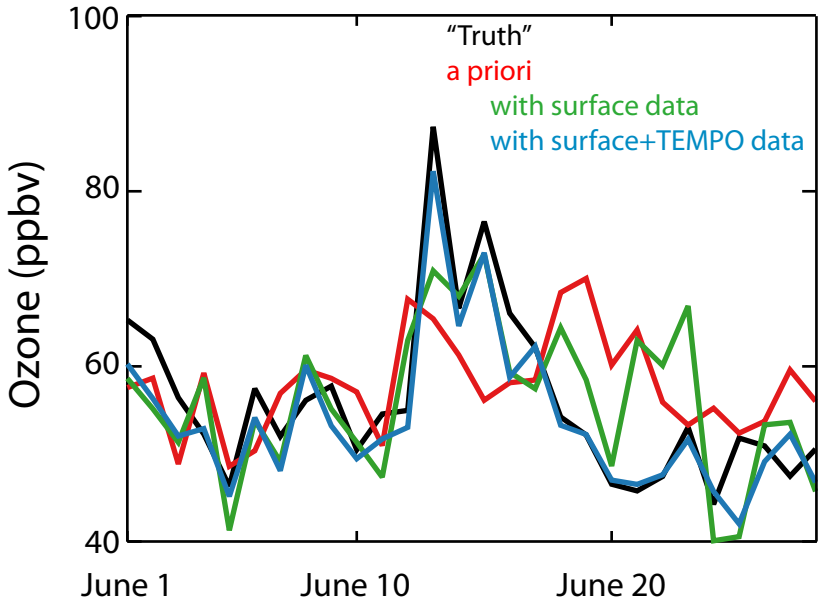

Figure 4.6: Detection of an exceptional ozone event by TEMPO. The Figure shows the June 2010 time series of daily maximum 8-h (MDA8) ozone concentrations at a location in northern New Mexico (107°W, 36°N) featuring a major stratospheric intrusion on June 13 in the AM3-Chem model taken as the "truth" (black line). The ability to capture this event is examined for the GEOS-Chem model without data assimilation (a priori, red line) and with assimilation of surface measurements only (green line) and satellite measurements added (blue line).

Evidence of free tropospheric origin for the June 13 event is critical to achieving an "exceptional event" designation. **Figure 4.7** (top left) shows a longitude-altitude cross section of ozone concentrations in the AM3-Chem model taken as the "truth". The stratospheric intrusion is manifest at 103-109°W. The *a priori* GEOS-Chem model (top right) also shows a stratospheric ozone enhancement extending to the surface but of much smaller magnitude. Assimilation of

surface measurements (not shown) makes little correction in the free troposphere. Satellite measurement imagery from TEMPO without assimilation (bottom left) shows elevated values in the free troposphere but does not properly represent surface gradients due to instrument smoothing. Assimilating TEMPO observations into the GEOS-Chem CTM together with LEO measurements (bottom right) captures the magnitude and spatial structure of the stratospheric intrusion, and this would make a strong case for diagnosis of an exceptional event.

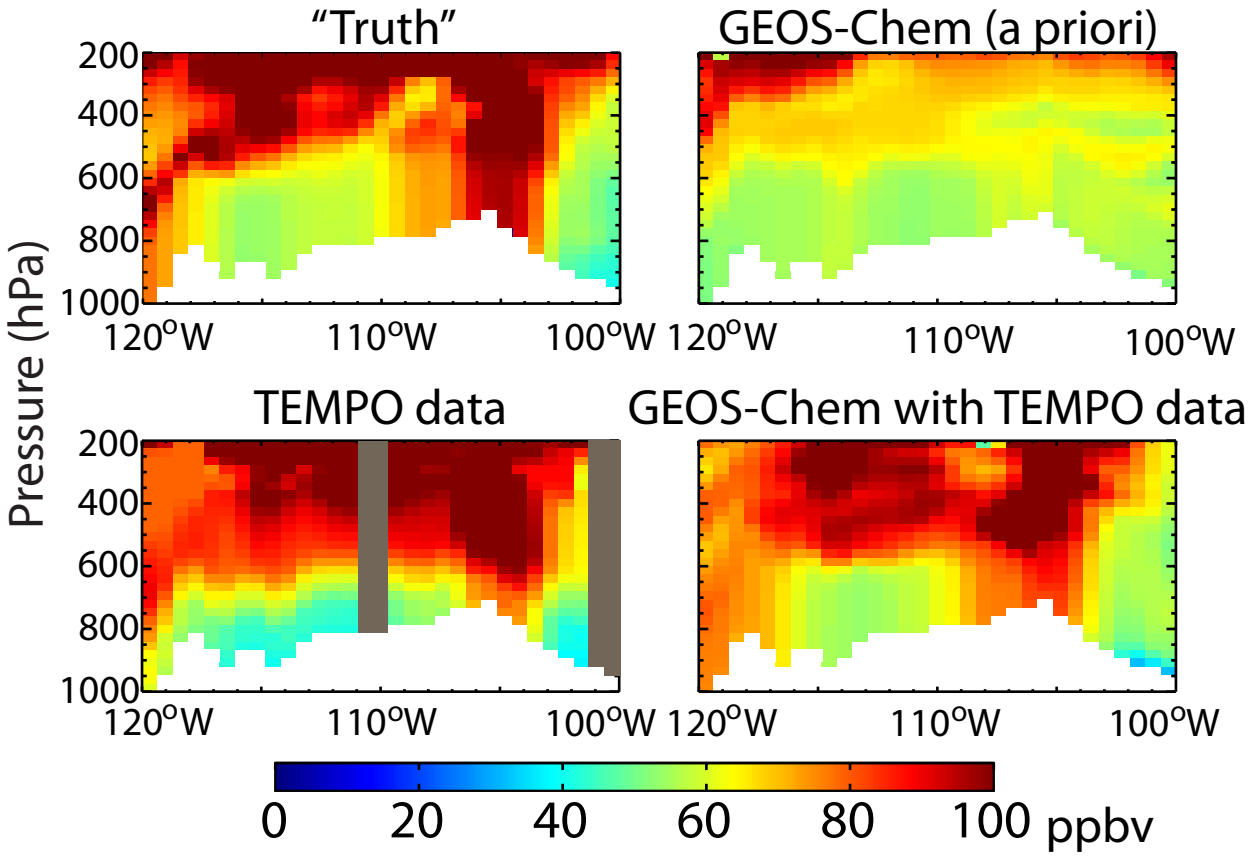

Figure 4.7: Longitude-altitude cross-section of ozone concentrations (36°N, 3 GMT on June 14, 2010) associated with the stratospheric intrusion of Figure 6. The "true" state from the AM3-Chem model (top left) is compared to the GEOS-Chem model without data assimilation (top right) and with assimilation of surface and satellite data (bottom right). The bottom left panel shows synthetic TEMPO observations of the "true" state (gray regions indicate cloudy scenes) without data assimilation. Local topography is shown in white.

We see here that the use of data assimilation efficiently enhances the information from TEMPO to constrain surface air concentrations. Information from the LEO instrument does not add significantly in this case to observations from TEMPO, although it does correct ozone fields over the ocean where TEMPO does not observe at night. The LEO instrument could thus be valuable for tracking transpacific transport of ozone plumes.

4.5 Summary

We demonstrated the potential of future TEMPO UV+Vis geostationary observations to monitor ozone exceedances in the Intermountain West and identify those exceedances caused by the North American background. Our goal was to inform the TEMPO observing strategy and develop methods for exploitation of its data. To accomplish this we performed an observation system simulation experiment (OSSE) for assimilation of the TEMPO data using two different chemical transport models (CTMs), one as the "true" atmosphere and one as the forward model for data assimilation. We also included in our OSSE surface measurements from the current CASTNet monitoring network sites in the Intermountain West (12 sites) and satellite measurements from a thermal infrared (TIR) low-elevation orbit (LEO) instrument projected to be in orbit concurrently with TEMPO.

An important factor in data assimilation is the scales over which observed information can be propagated with the forward model. We quantified this using model error correlation length scales for the Intermountain West based on actual CASTNet and ozonesonde data. We find length scales of 500 km (horizontal) and 1.7 km (vertical). These are in close agreement with error correlation length scales between the two CTMs used in our OSSE.

We find that the CASTNet surface observations are too sparse to adequately monitor high-ozone events in the Intermountain West even after data assimilation. We show that the TEMPO geostationary observations will provide a greatly improved observing system for monitoring such events. In addition, because of the information they provide on the vertical distribution of ozone, they can effectively diagnose NAAQS exceedances caused by background ozone. Concurrent LEO satellite observations provide no significant added value for monitoring the ozone background over the US but could be useful for tracking transpacific plumes.

Use of the complete observing system simulated here (surface, geostationary, and LEO) will provide a powerful tool for future air quality policy. Planning is underway to combine this system with regional air quality models to supply the public with near real time pollution reports and forecasts. These reports and forecasts would be much the same as currently available weather information, also provided in large part from geostationary satellite observations.

Acknowledgements: This work was supported by the NASA Earth Science Division and by a NASA Earth and Space Science Fellowship to Peter Zoogman.

References:

Arnold, C. and Dey, C., 1986. Observing-systems simulation experiments - past, present, and future. Bulletin of the American Meteorological Society 67, 687-695.

August, T., Klaes, D., Schluessel, P., Hultberg, T., Crapeau, M., Arriaga, A., O'Carroll, A., Coppens, D., Munro, R., Calbet, X., 2012. IASI on metop-A: Operational level 2 retrievals after five years in orbit. Journal of Quantitative Spectroscopy & Radiative Transfer 113, 1340-1371.

Bak, J., Kim, J.H., Liu, X., Chance, K., Kim, J., 2013. Evaluation of ozone profile and tropospheric ozone retrievals from GEMS and OMI spectra. Atmospheric Measurement Techniques 6, 239-249.

Bey, I., Jacob, D., Yantosca, R., Logan, J., Field, B., Fiore, A., Li, Q., Liu, H., Mickley, L., Schultz, M., 2001. Global modeling of tropospheric chemistry with assimilated meteorology: Model description and evaluation. Journal of Geophysical Research-Atmospheres 106, 23073-23095.

Brodin, M., Helmig, D., Oltmans, S., 2010. Seasonal ozone behavior along an elevation gradient in the colorado front range mountains. Atmospheric Environment 44, 5305-5315.

Chance, K., Lui, X., Suleiman, R.M., Flittner, D.E., Janz, S.J., 2012. Tropspheric Emissions: Monitoring of Pollution (TEMPO). Abstract A31B-0020 presented at the 2012 AGU Fall Meeting

Chance, K., Burrows, J., Perner, D., Schneider, W., 1997. Satellite measurements of atmospheric ozone profiles, including tropospheric ozone, from ultraviolet/visible measurements in the nadir geometry: A potential method to retrieve tropospheric ozone. Journal of Quantitative Spectroscopy & Radiative Transfer 57, 467-476.

Clerbaux, C., Boynard, A., Clarisse, L., George, M., Hadji-Lazaro, J., Herbin, H., Hurtmans, D., Pommier, M., Razavi, A., Turquety, S., Wespes, C., Coheur, P.-., 2009. Monitoring of atmospheric composition using the thermal infrared IASI/MetOp sounder. Atmospheric Chemistry and Physics 9, 6041-6054.

Cooper, O.R., Oltmans, S.J., Johnson, B.J., Brioude, J., Angevine, W., Trainer, M., Parrish, D.D., Ryerson, T.R., Pollack, I., Cullis, P.D., Ives, M.A., Tarasick, D.W., Al-Saadi, J., Stajner, I., 2011. Measurement of western US baseline ozone from the surface to the tropopause and assessment of downwind impact regions. Journal of Geophysical Research-Atmospheres 116, D00V03.

Cooper, O.R., Gao, R., Tarasick, D., Leblanc, T., Sweeney, C., 2012. Long-term ozone trends at rural ozone monitoring sites across the United States, 1990-2010. Journal of Geophysical Research-Atmospheres 117, D22307.

Edwards, D.P., Arellano, A.F., Jr., Deeter, M.N., 2009. A satellite observation system simulation experiment for carbon monoxide in the lowermost troposphere. Journal of Geophysical Research-Atmospheres 114, D14304.

Emery, C., Jung, J., Downey, N., Johnson, J., Jimenez, M., Yarvvood, G., Morris, R., 2012. Regional and global modeling estimates of policy relevant background ozone over the United States. Atmospheric Environment 47, 206-217.

Fiore, A., Jacob, D., Liu, H., Yantosca, R., Fairlie, T., Li, Q., 2003. Variability in surface ozone background over the United States: Implications for air quality policy. Journal of Geophysical Research-Atmospheres 108, 4787.

Fiore, A., Jacob, D., Bey, I., Yantosca, R., Field, B., Fusco, A., Wilkinson, J., 2002. Background ozone over the United States in summer: Origin, trend, and contribution to pollution episodes. Journal of Geophysical Research-Atmospheres 107, 4275.

Fishman, J., Iraci, L.T., Al-Saadi, J., Chance, K., Chavez, F., Chin, M., Coble, P., Davis, C., DiGiacomo, P.M., Edwards, D., Eldering, A., Goes, J., Herman, J., Hu, C., Jacob, D.J., Jordan, C., Kawa, S.R., Key, R., Liu, X., Lohrenz, S., Mannino, A., Natraj, V., Neil, D., Neu, J., Newchurch, M., Pickering, K., Salisbury, J., Sosik, H., Subramaniam, A., Tzortziou, M., Wang, J., Wang, M., 2012. The united states' next generation of atmospheric composition and coastal ecosystem measurements NASA's geostationary coastal and air pollution events (GEO-CAPE) mission. Bulletin of the American Meteorological Society 93, 1547-+.

Fu, D., Worden, J.R., Liu, X., Kulawik, S.S., Bowman, K.W., Natraj, V., 2013. Characterization of ozone profiles derived from aura TES and OMI radiances. Atmospheric Chemistry and Physics 13, 3445-3462.

Ingmann, P., Veihelmann, B., Langen, J., Lamarre, D., Stark, H., Courreges-Lacoste, G.B., 2012. Requirements for the GMES atmosphere service and ESA's implementation concept: Sentinels-4/-5 and-5p. Remote Sensing of Environment 120, 58-69.

Jaffe, D., 2011. Relationship between surface and free tropospheric ozone in the western U.S. Environmental science & technology 45, 432-438.

Jaffe, D.A. and Wigder, N.L., 2012. Ozone production from wildfires: A critical review. Atmospheric Environment 51, 1-10.

Kaynak, B., Hu, Y., Martin, R.V., Russell, A.G., Choi, Y., Wang, Y., 2008. The effect of lightning NOx production on surface ozone in the continental united states. Atmospheric Chemistry and Physics 8, 5151-5159.

Khattatov, B., Lamarque, J., Lyjak, L., Menard, R., Levelt, P., Tie, X., Brasseur, G., Gille, J., 2000. Assimilation of satellite observations of long-lived chemical species in global

chemistry transport models. Journal of Geophysical Research-Atmospheres 105, 29135-29144.

Langford, A.O., Aikin, K.C., Eubank, C.S., Williams, E.J., 2009. Stratospheric contribution to high surface ozone in colorado during springtime. Geophysical Research Letters 36, L12801.

Lefohn, A., Oltmans, S., Dann, T., Singh, H., 2001. Present-day variability of background ozone in the lower troposphere. Journal of Geophysical Research-Atmospheres 106, 9945-9958.

Lin, M., Fiore, A.M., Cooper, O.R., Horowitz, L.W., Langford, A.O., Levy,Hiram,,II, Johnson, B.J., Naik, V., Oltmans, S.J., Senff, C.J., 2012. Springtime high surface ozone events over the western United States: Quantifying the role of stratospheric intrusions. Journal of Geophysical Research-Atmospheres 117, D00V22.

Lin, M., Fiore, A.M., Horowitz, L.W., Cooper, O.R., Naik, V., Holloway, J., Johnson, B.J., Middlebrook, A.M., Oltmans, S.J., Pollack, I.B., Ryerson, T.B., Warner, J.X., Wiedinmyer, C., Wilson, J., Wyman, B., 2012. Transport of asian ozone pollution into surface air over the western United States in spring. Journal of Geophysical Research-Atmospheres 117, D00V07.

Liu, X., Sioris, C., Chance, K., Kurosu, T., Newchurch, M., Martin, R., Palmer, P., 2005. Mapping tropospheric ozone profiles from an airborne ultraviolet-visible spectrometer. Applied Optics 44, 3312-3319.

Lord, S.J., Kalnay E., Daley R., Emmitt G.D., Atlas R., 1997. Using OSSEs in the design of future g eneration integrated observing systems. Preprints, 1st Symposium on Integrated Observing Systems, Long Beach, CA, AMS, 45-47.

Mueller, S.F. and Mallard, J.W., 2011. Contributions of natural emissions to ozone and PM2.5 as simulated by the community multiscale air quality (CMAQ) model. Environmental science & technology 45, 4817-4823.

Natraj, V., Liu, X., Kulawik, S., Chance, K., Chatfield, R., Edwards, D.P., Eldering, A., Francis, G., Kurosu, T., Pickering, K., Spurr, R., Worden, H., 2011. Multi-spectral sensitivity studies for the retrieval of tropospheric and lowermost tropospheric ozone from simulated clear-sky GEO-CAPE measurements. Atmospheric Environment 45, 7151-7165.

Parrington, M., Jones, D.B.A., Bowman, K.W., Horowitz, L.W., Thompson, A.M., Tarasick, D.W., Witte, J.C., 2008. Estimating the summertime tropospheric ozone distribution over North America through assimilation of observations from the tropospheric emission spectrometer. Journal of Geophysical Research-Atmospheres 113, D18307.

Reid, N., Yap, D., Bloxam, R., 2008. The potential role of background ozone on current and emerging air issues: An overview. Air Quality Atmosphere and Health 1, 19-29.

Rodgers, C.D., 2000. Inverse Methods for Atmospheric Sounding. World Scientific, River Edge, New Jersey,

Singh, H.B., Cai, C., Kaduwela, A., Weinheimer, A., Wisthaler, A., 2012. Interactions of fire emissions and urban pollution over california: Ozone formation and air quality simulations. Atmospheric Environment 56, 45-51.

United States Environmental Protection Agency, 2010. Clean air status and trends network second quarter 2010 quality assurance report.

United States Environmental Protection Agency, 2012. Welfare Risk and Exposure Assessment for Ozone.

United States Environmental Protection Agency, 2013. Interim Guidance to Implement Requirements for the Treatment of Air Quality Monitoring Data Influenced by Exceptional Events.

Worden, H.M., Deeter, M.N., Frankenberg, C., George, M., Nichitiu, F., Worden, J., Aben, I., Bowman, K.W., Clerbaux, C., Coheur, P.F., de Laat, A.T.J., Detweiler, R., Drummond, J.R., Edwards, D.P., Gille, J.C., Hurtmans, D., Luo, M., Martinez-Alonso, S., Massie, S., Pfister, G., Warner, J.X., 2013. Decadal record of satellite carbon monoxide observations. Atmospheric Chemistry and Physics 13, 837-850.

Yates, E.L., Iraci, L.T., Pierce, R.B., Johnson, M.S., Reddy, P.J., Tadic, J.M., Loewenstein, M., Gore, W., 2013. Airborne observations and modeling of springtime stratosphere-to-troposphere transport over California. Atmos. Chem. Phys. Discuss. 13,

Zhang, L., Jacob, D.J., Liu, X., Logan, J.A., Chance, K., Eldering, A., Bojkov, B.R., 2010. Intercomparison methods for satellite measurements of atmospheric composition: Application to tropospheric ozone from TES and OMI. Atmospheric Chemistry and Physics 10, 4725-4739.

Zhang, L., Jacob, D.J., Boersma, K.F., Jaffe, D.A., Olson, J.R., Bowman, K.W., Worden, J.R., Thompson, A.M., Avery, M.A., Cohen, R.C., Dibb, J.E., Flock, F.M., Fuelberg, H.E., Huey, L.G., McMillan, W.W., Singh, H.B., Weinheimer, A.J., 2008. Transpacific transport of ozone pollution and the effect of recent Asian emission increases on air quality in North America: An integrated analysis using satellite, aircraft, ozonesonde, and surface observations. Atmospheric Chemistry and Physics 8, 6117-6136.

Zhang, L., Jacob, D.J., Downey, N.V., Wood, D.A., Blewitt, D., Carouge, C.C., van Donkelaar, A., Jones, D.B.A., Murray, L.T., Wang, Y., 2011. Improved estimate of the policy-relevant background ozone in the United States using the GEOS-chem global model with 1/2 degrees x 2/3 degrees horizontal resolution over North America. Atmospheric Environment 45, 6769-6776.

Zoogman, P., Jacob, D.J., Chance, K., Worden, H.M., Edwards, D.P., Zhang, L., 2013. Improved monitoring of surface ozone air quality by joint assimilation of geostationary satellite observations of ozone and CO. submitted to Atmos. Environ.

Zoogman, P., Jacob, D.J., Chance, K., Zhang, L., Le Sager, P., Fiore, A.M., Eldering, A., Liu, X., Natraj, V., Kulawik, S.S., 2011. Ozone air quality measurement requirements for a geostationary satellite mission. Atmospheric Environment 45, 7143-7150.